RESEARCH ARTICLE

Input–output connections of LJA5 prodynorphin neurons

Lindsay J. Agostinelli[1,2,4] ⓘ | Madison R. Mix[2] | Marco M. Hefti[3] ⓘ |
Thomas E. Scammell[4] | Alexander G. Bassuk[1,2]

[1]Department of Neurology, Roy J. and Lucille A. Carver College of Medicine, The University of Iowa, Iowa City, Iowa

[2]Department of Pediatrics, University of Iowa, Iowa City, Iowa

[3]Department of Pathology, University of Iowa, Iowa City, Iowa

[4]Department of Neurology, Beth Israel Deaconess Medical Center and Harvard Medical School, Boston, Massachusetts

Correspondence
Alexander G. Bassuk, Professor, Stead Family Chair in Pediatric Neurology, Division Director, Child Neurology, Neurology, Genetics, Molecular and Cellular Biology, the Iowa Neuroscience Institute (INI), and the Medical Scientist Training Program, University of Iowa, 25 S. Grand Ave, 2040 Medical Laboratories, Iowa City, IA 52242-1009.
Email: alexander-bassuk@uiowa.edu

Abstract

Sensory information is transmitted from peripheral nerves, through the spinal cord, and up to the brain. Sensory information may be modulated by projections from the brain to the spinal cord, but the neural substrates for top-down sensory control are incompletely understood. We identified a novel population of inhibitory neurons in the mouse brainstem, distinguished by their expression of prodynorphin, which we named LJA5. Here, we identify a similar group of *Pdyn+* neurons in the human brainstem, and we define the efferent and afferent projection patterns of LJA5 neurons in mouse. Using specific genetic tools, we selectively traced the projections of the *Pdyn*-expressing LJA5 neurons through the brain and spinal cord. Terminal fields were densest in the lateral and ventro-lateral periaqueductal gray (PAG), lateral parabrachial nucleus (LPB), caudal pressor area, and lamina I of the spinal trigeminal nucleus and all levels of the spinal cord. We then labeled cell types in the PAG, LPB, medulla, and spinal cord to better define the specific targets of LJA5 boutons. LJA5 neurons send the only known inhibitory descending projection specifically to lamina I of the spinal cord, which transmits afferent pain, temperature, and itch information up to the brain. Using retrograde tracing, we found LJA5 neurons receive inputs from sensory and stress areas such as somatosensory/insular cortex, preoptic area, paraventricular nucleus, dorsomedial nucleus and lateral hypothalamus, PAG, and LPB. This pattern of inputs and outputs suggest LJA5 neurons are uniquely positioned to be activated by sensation and stress, and in turn, inhibit pain and itch.

KEYWORDS

anterograde tracing, brainstem, dynorphin, human, lamina I, mouse, retrograde tracing, RRID AB_10013220, RRID AB_11180610, RRID AB_11213126, RRID AB_2107133, RRID AB_2536611

1 | INTRODUCTION

Chronic pain and itch comprise a large clinical burden (Mansfield, Sim, Jordan, & Jordan, 2016; Schaefer et al., 2014; Yosipovitch & Bernhard, 2013), and there are many investigations into the neurocircuitry underlying these sensations. Most research has focused on the neural control of pain and itch via the "bottom-up" pathway, where sensory information is transmitted from skin to lamina I of the spinal cord, and up to the brain (Craig, 2002; Dong & Dong, 2018). However, it is not well understood how the brain modulates pain and itch sensations in a "top-down" fashion.

We recently discovered a group of inhibitory brainstem neurons with projections specifically to the sensory region of the spinal cord (lamina I). We named these neurons LJA5 to describe their location in the *lateral pons, juxta A5* (the noradrenergic cell group). These LJA5 neurons are distinguished by their prodynorphin expression. Prodynorphin is the precursor to dynorphin, an inhibitory opioid neuropeptide expressed in numerous brain and spinal cord regions (Waldhoer, Bartlett, & Whistler, 2004). Previous studies characterizing *Pdyn* expression and dynorphin distribution throughout the rat brain failed to comment on these ventral brainstem neurons (LJA5), although a few prodynorphin/dynorphin-expressing neurons can be seen around the facial nerve in previously published figures (Fallon & Leslie, 1986; Merchenthaler, Maderdrut, Cianchetta, Shughrue, & Bronstein, 1997).

Here, we sought to characterize the efferent and afferent projections of LJA5 in relation to known cell types in the brainstem. We then investigated the neurochemical cell types innervated by the LJA5 neurons. Additionally, we analyzed human tissue to determine if this cell group is present in the human brainstem.

2 | METHODS

2.1 | Animals

To generate dynorphin reporter mice, we crossed *Pdyn-IRES-Cre* mice with R26-lsl-L10-GFP mice, two lines of mice that were produced and characterized in the Lowell lab and were published previously (Krashes et al., 2014). The *Pdyn-IRES*-Cre mice are available from The Jackson Laboratory (stock no. 027958). *Pdyn-IRES*-Cre mice selectively express Cre recombinase in cells that have expressed prodynorphin, and L10-GFP mice have a loxP-flanked STOP cassette which prevents the transcription of downstream green fluorescent protein (GFP). We crossed these mice with *Pdyn-IRES*-Cre mice because in the presence of Cre recombinase, the STOP cassette is deleted, resulting in offspring that express GFP selectively in Cre-expressing dynorphin cells, creating *Pdyn*-GFP reporter mice.

We housed all mice on a 12:12 light: dark cycle with lights on at 0600 at 22°C ambient temperature with ad libitum access to food and water. All protocols and care of the mice followed National Institute of Health guidelines and were approved by the University of Iowa Institutional Animal Care and Use Committee.

2.2 | Surgery/microinjections

We used Cre-conditional anterograde tracing to map projections of the LJA5 neurons. We injected the LJA5 region of Cre-expressing mice (*Pdyn*-GFP mice) (10–11 weeks old, male and female) with an adeno-associated viral vector (AAV8-EF1α-DIO-hChR2[H134R]-mCherry, 6×10^{12} pfu/ml, UNC Vector Core) coding for Cre-dependent channelrhodopsin (ChR2) tagged with the red fluorescent protein mCherry (AAV-DIO-ChR2-mCherry) (*n* = 3 mice), or an adeno-associated viral vector AAV8-hEF1α-DIO-synaptophysin-mCherry, 2.5×10^{13} vg/ml, developed by Dr Rachel Neve at the Massachusetts Institute of Technology McGovern Institute for Brain Research Viral Vector Core) coding for Cre-dependent synaptophysin tagged with the red fluorescent protein mCherry (AAV-DIO-synaptophysin-mCherry) (*n* = 4 mice). In these AAVs, the ChR2-mCherry or synaptophysin-mCherry sequence is inverted and surrounded by pairs of loxP and lox2722 sites, thus limiting synaptophysin-mCherry or hM3Dq-mCherry expression to cells that contain Cre recombinase. By injecting this AAV into mice that express Cre recombinase selectively in prodynorphin-expressing neurons, we restricted synaptophysin-mCherry or hM3Dq-mCherry expression to LJA5 dynorphinergic neurons.

For retrograde tracing, we used cholera toxin subunit b (CTb) (List Biological, Campbell, California; 0.1% in saline) (*n* = 4 mice).

For stereotaxic delivery of these tracers, we first anesthetized mice with ketamine/xylazine (100/10 mg/kg. i.p.) and unilaterally microinjected 90 nl of AAV or 16 nl of CTb into the LJA5 region of the hindbrain (coordinates from bregma: AP ‑4.83 mm, RL 1.35 mm, DV ‑5.50 mm from the top of the skull).

We perfused the mice 1 week after CTb injection and 4 weeks after AAV injection. Specifically, we deeply anesthetized mice with ketamine/xylazine (150/15 mg/kg i.p.) and transcardially perfused them with 50 ml phosphate-buffered saline (PBS; pH 7.4) followed by 50 ml of buffered 10% formalin (pH 7.0; Fisher Scientific, Fair Lawn, NJ). We removed and postfixed the brains and spinal cords for 12 hr in 10% formalin and then cryoprotected them in PBS containing 20% sucrose. We later sectioned the brains and spinal cords at 30 μm into a 1:4 series on a freezing microtome.

2.3 | Histology

All brains for tracing were perfused and sectioned as described earlier. We perfused four additional *Pdyn*-GFP mice without stereotaxic microinjections for immunohistochemistry (IHC) and RNAscope in situ hybridization. Detailed information on all primary antisera used in these experiments are listed in Table 1. To visualize the injection sites of AAV anterograde tracers, one series of each brain was incubated overnight in rat anti-mCherry (1:2,000; Life Technologies; M112171; RRID AB_2536611) and chicken anti-GFP (1:5,000; Invitrogen; A10262; RRID AB_11180610) followed by 1 hr incubation in donkey anti-rat IgG conjugated to Cy3 (1:500; Jackson ImmunoResearch; 712-165-153) and donkey anti-chicken IgG conjugated to Alexa

TABLE 1 Details on antisera used in these experiments

Antigen	Immunogen	Manufacturer, catalog or lot number, the RRID species, mono or poly	Concentration
mCherry	Full length mCherry protein	Life Technologies/Invitrogen, Cat# M11217, RRID AB_2536611, rat, monoclonal	1:5,000 for DAB, 1:2,000 for fluorescence
GFP	GFP from *Aequorea victoria*	Life Technologies, A10262, RRID AB_11180610, chicken, polyclonal	1:5,000
Forkhead box protein 2 (FoxP2)	Recombinant peptide sequence corresponding to Ala640-Glu715 of human FoxP2	R and D Systems, Cat # AF5647, RRID AB_2107133, sheep, polyclonal	1:3,000
Tyrosine hydroxylase (TH)	Native tyrosine hydroxylase from rat pheochromocytoma	Millipore, sheep polyclonal, Cat# AB1542, RRID: AB_11213126	1:2,000
Cholera toxin B subunit (CTb)	Purified choleragenoid, the B subunit of cholera toxin	List Biologicals, Cat# 703, RRID AB_10013220, goat, polyclonal	1:15,000 for DAB, 1:5,000 for fluorescence

488 (1:500; Jackson ImmunoResearch; 703-065-155). In addition to labeling GFP and mCherry, we incubated sections containing the parabrachial nucleus or caudal medulla (A1) with a third antibody, sheep anti-FoxP2 IgG (1:3,000; R&D Systems; AF5647; RRID AB_2107133) or rabbit anti-tyrosine hydroxylase (TH) IgG (1:2,000; Millipore; AB152; RRID AB_11213126), respectively, followed by 1 hr incubation in donkey anti-sheep IgG conjugated to Cy5 (1:500; Jackson ImmunoResearch; 713-175-147) or donkey anti-rabbit IgG conjugated to Cy5 (1:500; Jackson ImmunoResearch; 711-175-152). The GFP, mCherry, and CTb antisera produced no labeling in wild-type mice lacking these peptides/tracers. The TH and FoxP2 antisera produced labeling that reflected well established protein and mRNA distributions seen in our previous analyses and those of our colleagues (Agostinelli, Geerling, & Scammell, 2019; Verstegen, Vanderhorst, Gray, Zeidel, & Geerling, 2017) the Allen Brain Atlas (http://www.brain-map.org) and references from our Discussion section. Additionally, manufacturers performed Western blots of brain tissue extracts with these antisera and found a single band at ~62 kDa corresponding to TH and ~90 kDa corresponding to FoxP2, along with specificity for mouse and human tyrosine hydroxylase and FoxP2.

We used in situ hybridization to label PAG sections for preprotachykinin-1 (*Tac1*) mRNA. We used a probe directed against mouse *Tac1* (410351-C2) and the RNAscope multiplex V1 fluorescent assay (Advanced Cell Diagnostics). We then labeled these sections for mCherry to visualize LJA5 boutons using the IHC staining method described earlier.

For these AAV anterograde tracing cases, we then stained a second series of full brain and spinal cord sections to visualize axonal projections and terminal fields with DAB. We placed sections into 0.3% hydrogen peroxide for 30 min and then incubated them overnight in rat anti-mCherry (1:5,000). We then placed sections in biotinylated donkey anti-rat secondary antisera (1:500; Jackson ImmunoResearch; 712-066-153) followed by 1 hr in avidin-biotin complex (Vectastain ABC Elite Kit; Vector Laboratories). We labeled mCherry black with DAB in tris-buffered saline (TBS) containing 0.024% hydrogen peroxide and 0.2% ammonium nickel (II) sulfate (Sigma).

For CTb studies, we also stained the first series with double fluorescence to visualize the CTb injection site. We incubated the hindbrain overnight in goat-anti CTb (1:5,000; List Biologicals; 703; RRID AB_10013220) and chicken anti-GFP followed by 1 hr incubation of donkey anti-goat IgG conjugated to Alexa 555 (1:500; Invitrogen; A21432) and donkey anti-chicken IgG conjugated to Alexa 488.

We then stained a second full series of CTb tracing cases with DAB. We placed sections into 0.3% hydrogen peroxide for 30 min and then incubated them overnight in goat-anti CTb (1:15,000). We then placed sections in biotinylated donkey anti-goat secondary antisera (1:500; Jackson ImmunoResearch; 705-065-147) followed by 1 hr in avidin-biotin complex. We labeled mCherry black with DAB in tris-buffered saline (TBS) containing 0.024% hydrogen peroxide and 0.2% ammonium nickel (II) sulfate (Sigma).

After immunolabeling, we mounted and dried sections on Superfrost Plus slides. For sections with fluorescence immunolabeling, we coverslipped with fade-retardant mounting medium containing DAPI (Vectashield; Vector Labs). For DAB-labeled tissue, we dehydrated sections in graded ethanols and cleared them in xylenes before coverslipping with a toluene-based mounting media (Cytoseal; Thermo Scientific). We acquired whole-slide images using a slide-scanning microscope (Olympus VS120) and reviewed slides in OlyVIA software (Olympus). After DAB sections were imaged, we removed the coverslips and Nissl stained the sections in thionin for 30 s, followed by graded ethanol washes.

2.4 | Validation of neurochemical specificity

Pdyn-GFP mice were validated previously (Geerling et al., 2016; Krashes et al., 2014). To confirm that GFP expression was limited to prodynorphin-expressing neurons in the LJA5 region, we performed in situ hybridization with RNAscope using a probe directed against mouse *Pdyn* (318771, Advanced Cell Diagnostics) and the RNAscope multiplex V1 fluorescent assay.

In addition, we performed double in situ hybridization using the *Pdyn* probe and another probe directed against mouse *Gad1* (glutamic acid decarboxylase 1; probe 400951, Advanced Cell Diagnostics) with RNAscope multiplex V2 fluorescent assay.

We then used the same assay on LJA5 sections to double label *Pdyn* with gastrin-releasing peptide (l*Grp*) (317861-C2, Advanced Cell Diagnostics).

2.5 | Analysis of injection sites

To measure the specificity of neuronal transduction, we immuno-stained sections for GFP and mCherry (to further label the native GFP of reporter neurons and mCherry of the AAVs) and counted the number of GFP+ cells that expressed mCherry across all sections containing LJA5 neurons (spanning typically 6 axial sections from a 1:4 series through the rostral hindbrain).

Analysis of AAV-DIO-synaptophysin-mCherry injection sites revealed that 97.9% of LJA5 GFP+ cells expressed mCherry. All mCherry cells were colocalized with GFP. For AAV-DIO-ChR2-mCherry, mCherry was expressed in a mean of 61.7% of LJA5 GFP+ neurons.

For retrograde tracing, we selected cases where CTb covered most of LJA5 neurons without extension into nearby structures such as the superior olivary complex (SOC). The diameter of the injection site was approximately 250 μm ML and approximately 600 μm AP.

2.6 | Analysis of anterograde tracing

To analyze projections, we used OlyVia software to view whole-slide images containing every section in the series. To quantify the density of axon terminals in various nuclei, independent, blinded observers used a qualitative scoring system of 0–3 with 0 = no axon terminals, 1 = a few axons terminals, 2 = moderate density of axon terminals, 3 = heavy density of axon terminals. Table 2 lists all regions with LJA5 axon terminals, plus a few relevant regions that did not contain labeled axons.

Drawings of anterograde tracing are derived from the case with the highest percentage of transduced LJA5 neurons (LJA-122). We used OlyVia software to select sections that had dense axonal labeling, and we included sections that had labeling in the most rostral and caudal regions. We placed images of sections from OlyVia into Adobe Illustrator, and we drew over every axon. We used Nissl images to draw boundaries of relevant landmarks.

To investigate LJA5 terminal fields, we analyzed synaptophysin anterograde tracing cases. We used fluorescent immunohistochemistry and in situ hybridization to label neuronal populations within LJA5 terminal fields.

2.7 | Analysis of retrograde tracing

To analyze the afferent projections to LJA5, we used OlyVia software to view whole-slide images containing every section in the series. To

TABLE 2 Labeling from anterograde and retrograde tracing from LJA5

Anterograde	
LPAG	2–3
Superior colliculus	1
Lateral lemniscus	1*
LPB	3
Contralateral LJA5	2
Parvicellular reticular nucleus (alpha)	2*
Pontine reticular nucleus caudal	1*
MPB	1
Int. reticular nucleus	1
NTS	1/2
Medullary reticular nuc	1–2
CPA	2
Spinal trigeminal	3
Lamina 1	3
Lateral spinal nucleus	3
Retrograde	
ACC/MO	2
Insular/somatosensory cortex	2
Preoptic (MPO/LPO)	2
BNST (ventral)	2
PVH	2
CEA	2
LHA	2
Preparasubthalamic	2
Zona incerta	2
DMH	2
STN	2
PAG	3
Midbrain reticular nucleus	2
Superior Colliculus	2
LPB	3
MPB	1
Inferior colliculus	1
Principle sensory nucleus of trigeminal	2
Med ret form: IRN	1
Med ret form: GRN	1–2
NTS	1–2
CPA	1–2
Spinal trigeminal nuc	1

Notes: 1 denotes scarce anterograde or retrograde labeling, 2 denotes moderate labeling, and 3 denotes dense labeling. Slash denotes variability between cases. Asterix denotes axons only (scarce boutons).

quantify the relative densities of retrogradely labeled cells, independent, blinded observers used a semi-quantitative scoring system of 0–3 with 0 = no CTb + cells, 1 = <25 CTb + cells, 2 = 25 – 100 CTb +

cells, 3 = >100 CTb + cells in a given structure (on the brain section with the most labeling for that structure). Table 2 lists all regions with CTb + cells.

To create drawings of retrograde tracing, we selected the case in which CTb was mostly limited to the LJA5 region (LJA-145). We used OlyVia software to select sections that had the most retrogradely labeled cells, and some sections between for completeness. We placed images of sections from OlyVia into Adobe Illustrator, and placed a blue circle on every CTb labeled cell. We used Nissl images to draw boundaries around relevant landmarks.

2.8 | Human tissue histology and labeling

Two infant brainstems were provided by neuropathologist Marco Hefti, MD. The first was from a 35 week gestation female (cause of death was autosomal recessive polycystic kidney disease 72 hr following birth, post-mortem interval was 40 hr). The other brainstem was donated from a 41-week gestation female (cause of death was meconium aspiration 24 hr after birth, with a post-mortem interval of 21 hr.) Brainstems were postfixed in 10% formalin for approximately 10 days. The brainstems were embedded in paraffin, cut in 10 μm sections, and mounted on Superfrost Plus slides. To deparaffinize the tissue prior to staining, the slides were baked at 70°C, cleared in xylenes, dehydrated in 100% ethanol, and air dried.

To appreciate the cytoarchitecture of the LJA5 region, Nissl staining with thionin was performed. After staining, we dehydrated sections in graded ethanols and cleared in xylenes before coverslipping with a toluene-based mounting media (Cytoseal; Thermo Scientific).

To assess the chemoarchitecture of the LJA5 region, we first performed single in situ hybridization using a human-specific probe for Pdyn (318771, Advanced Cell Diagnostics) RNAscope 2.5 HD Assay-Red followed by counterstain in hematoxylin. We then performed double in situ hybridization using human-specific probes for Pdyn (507161-C2) and Gad1 (465261-C1) with the RNAscope multiplex V2 fluorescent assay. Pdyn was labeled with Cy3 and Gad1 was labeled with Cy5. To distinguish LJA5 neurons from the A5 adrenergic cell group, we immunolabeled sections after in situ hybridization with rabbit anti-tyrosine hydroxylase (TH) (1:1,000; Millipore; AB152), in an overnight incubation followed by a 1-hr incubation in rabbit anti-Cy2 (1:500; Jackson ImmunoResearch; 711-225-152). Coverslipping was performed with a toluene-based mounting media (Cytoseal; Thermo Scientific) for 2.5 HD Assay-Red treated tissue or a fade-retardant mounting medium containing DAPI (Vectashield; Vector Labs) for fluorescently labeled tissue.

Finally, we imaged and analyzed images using the tools described earlier with mouse tissue. To create visual representations of LJA5 neurons, we placed images of sections from OlyVIA into Adobe Illustrator, and placed a green circle on every Pdyn labeled cell. We used details from DAPI and adjacent Nissl images to draw boundaries around relevant neuroanatomical landmarks.

3 | RESULTS

3.1 | LJA5 neuronal markers

3.1.1 | LJA5 neuronal markers in mouse

The LJA5 neurons are located in the ventrolateral brainstem, just dorsal to the SOC and rostral to the facial nerve exit (Figures 1 and 2). They are defined by their expression of Pdyn, the gene coding for prodynorphin, the precursor protein for the inhibitory opioid neuropeptide dynorphin.

We performed double in situ hybridization for Pdyn and Gad1 (glutamic acid decarboxylase 1, found in GABAergic neurons), and all of the Pdyn+ neurons expressed Gad1 (Figure 1c). There were many Gad1+ neurons that did not express Pdyn.

LJA5 neurons are separate from (but next to) the catecholaminergic group A5 as they do not express tyrosine hydroxylase (Figure 1d).

Next, we performed double in situ hybridization for Pdyn and Grp mRNA (gastrin releasing peptide) (Figure 3) because in this region, the Grp expression pattern is clustered similarly to Pdyn. We found that 71.2% ± 3.7 of LJA5 Pdyn+ neurons also express Grp, and 74.9% ± 6.2 of Grp+ neurons in the LJA5 region express Pdyn. In general, the Pdyn+/Grp- neurons had lower levels of Pdyn expression than the Pdyn+/Grp+ neurons. The Grp+/Pdyn- neurons were much smaller than the Pdyn+ neurons, and they were located dorsal or lateral to the Pdyn+ cluster.

3.1.2 | LJA5 in human brain

To map LJA5 neurons in human tissue, brainstem sections spanning from midbrain to medulla were sectioned, stained, and analyzed. This revealed a novel population of Pdyn-expressing neurons that span through the pons in the human brainstem (Figure 2a,b). The surrounding landmarks of these Pdyn neurons in human parallel the location of LJA5 neurons in the mouse brainstem (Figure 1). Nissl staining was first performed to determine section level on the rostral-caudal axis (Figure 2b). We used fluorescent in situ hybridization to identify Pdyn-expressing neurons in adjacent sections. LJA5 Pdyn-expressing neurons spanned rostrally from the level of the locus coeruleus (LC) and SOC, and caudally to the CN VII nucleus. Within this rostral-caudal span, LJA5 neurons specifically resided dorsal to the SOC, ventral to the CN V and VI nuclei, lateral to the CN VI nerve, and medial to the CN VII nerve (Figure 2a,b). LJA5 neurons exhibit clear punctate labeling for Pdyn mRNA (Figure 2c). Of importance, colocalization of Pdyn with Gad1-expressing neurons established that LJA5 neurons are GABAergic in the human brainstem (Figure 2d) as in mouse (Figure 1c). Furthermore, subsequent immunohistochemistry confirmed that LJA5 neurons are separate from and adjacent to the A5 catecholaminergic group as they do not express tyrosine hydroxylase (TH) (Figure 2e). Thus, similar to the mouse LJA5 neurons, the LJA5 group in human brainstem is GABAergic and adjacent to A5.
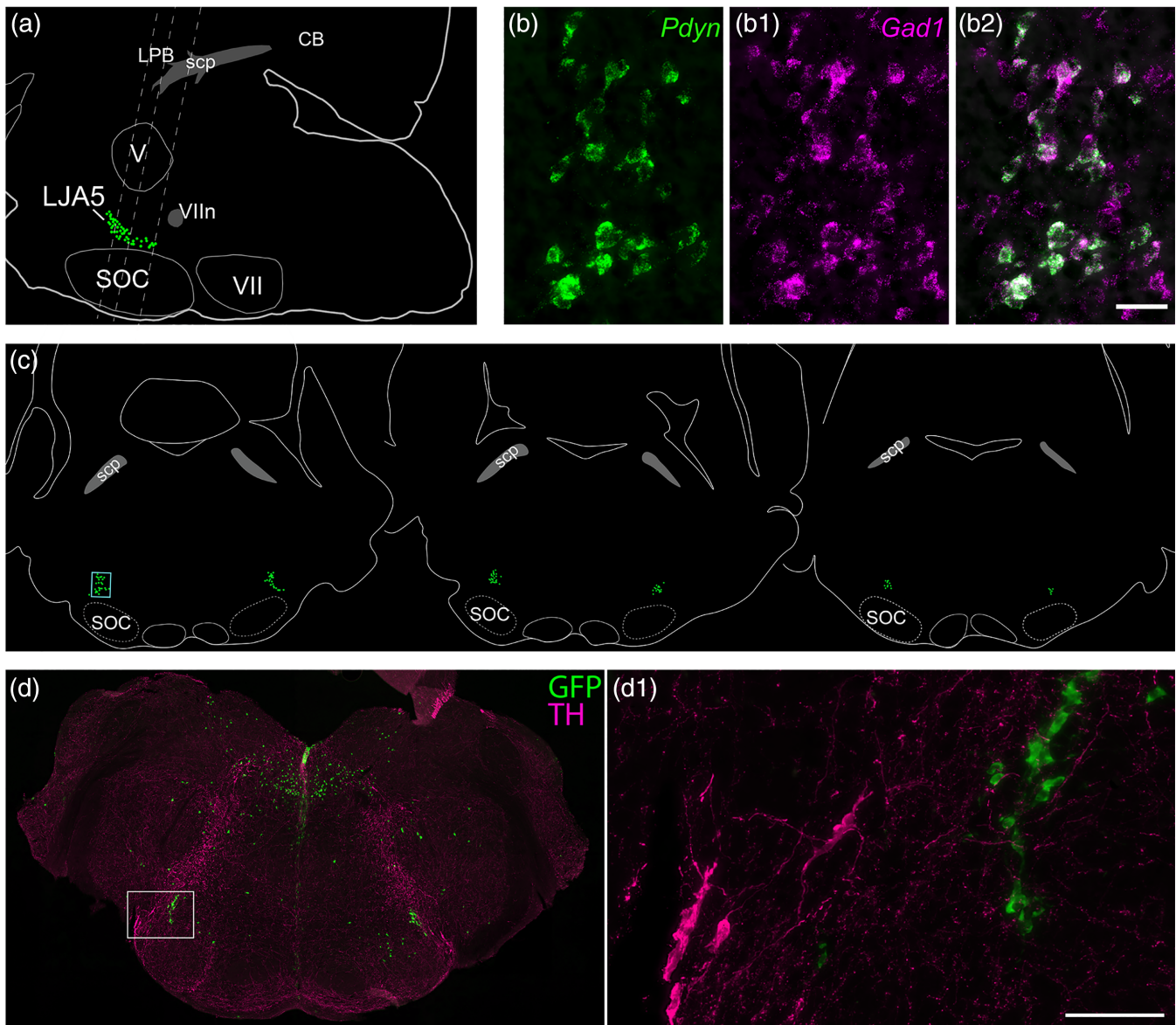
FIGURE 1 LJA5 is a novel population of prodynorphin-expressing, GABAergic neurons in the mouse ventrolateral pons. (a) Sagittal section through a *Pdyn*-GFP mouse (focusing on *Pdyn*+ neurons only in the LJA5 region). LJA5 neurons (GFP) are a cluster of prodynorphin neurons in the caudal ventrolateral pons, dorsal to the superior olivary complex (SOC) and just rostral to the facial nerve (VIIn). Dotted lines indicate the levels of the coronal sections shown in (c). (b) Double in situ hybridization reveals that prodynorphin mRNA (*Pdyn*, green) colocalizes (white) with mRNA for glutamic acid decarboxylase (*Gad1*, purple) (scale bar is 50 μm). These neurons are from a section that is drawn in (b). (c) Coronal sections of LJA5 *Pdyn*+ neurons in rostrocaudal distribution (focusing on *Pdyn*+ neurons only in the LJA5 region). Small blue box in first section is shown at high power in panel (b). (d) Coronal section from *Pdyn*-GFP mouse cut at a steep angle to reveal LJA5 GFP+ neurons in the same section as more caudal A5 tyrosine hydroxylase (TH) expressing neurons. LJA5 neurons lack TH and are dorsomedial to A5 (scale bar is 100 μm) [Color figure can be viewed at wileyonlinelibrary.com]

3.2 | LJA5 efferent projections

We injected Cre-dependent AAV-DIO-ChR2-mCherry into the ventrolateral brainstem of *Pdyn*-GFP mice, and histology of the injection sites revealed that mCherry expression was limited to the LJA5 neurons (Figure 4), a GFP+ cluster of neurons that are immediately rostral to the facial nerve exit. AAV-DIO-ChR2-mCherry robustly labeled the soma, axons, and terminals of *Pdyn*-expressing neurons in the injection site.

Axons projecting from LJA5 neurons arched rostral and traveled dorsally in the lateral lemniscus (ll) up to the periaqueductal gray (PAG) (Figure 5a) which is the most rostrally targeted structure of LJA5 neurons. Additionally, axons travel caudally to the lateral parabrachial nucleus (LPB) (Figure 5d). From there, axons traveled ventrally through the medulla to the A1 region and caudal pressor area (CPA) (Figure 5f), and robustly innervated the spinal trigeminal nucleus and tract (Figure 5g). Axons continued down through the entire spinal cord, densely innervating lamina I and the lateral spinal nucleus at every level
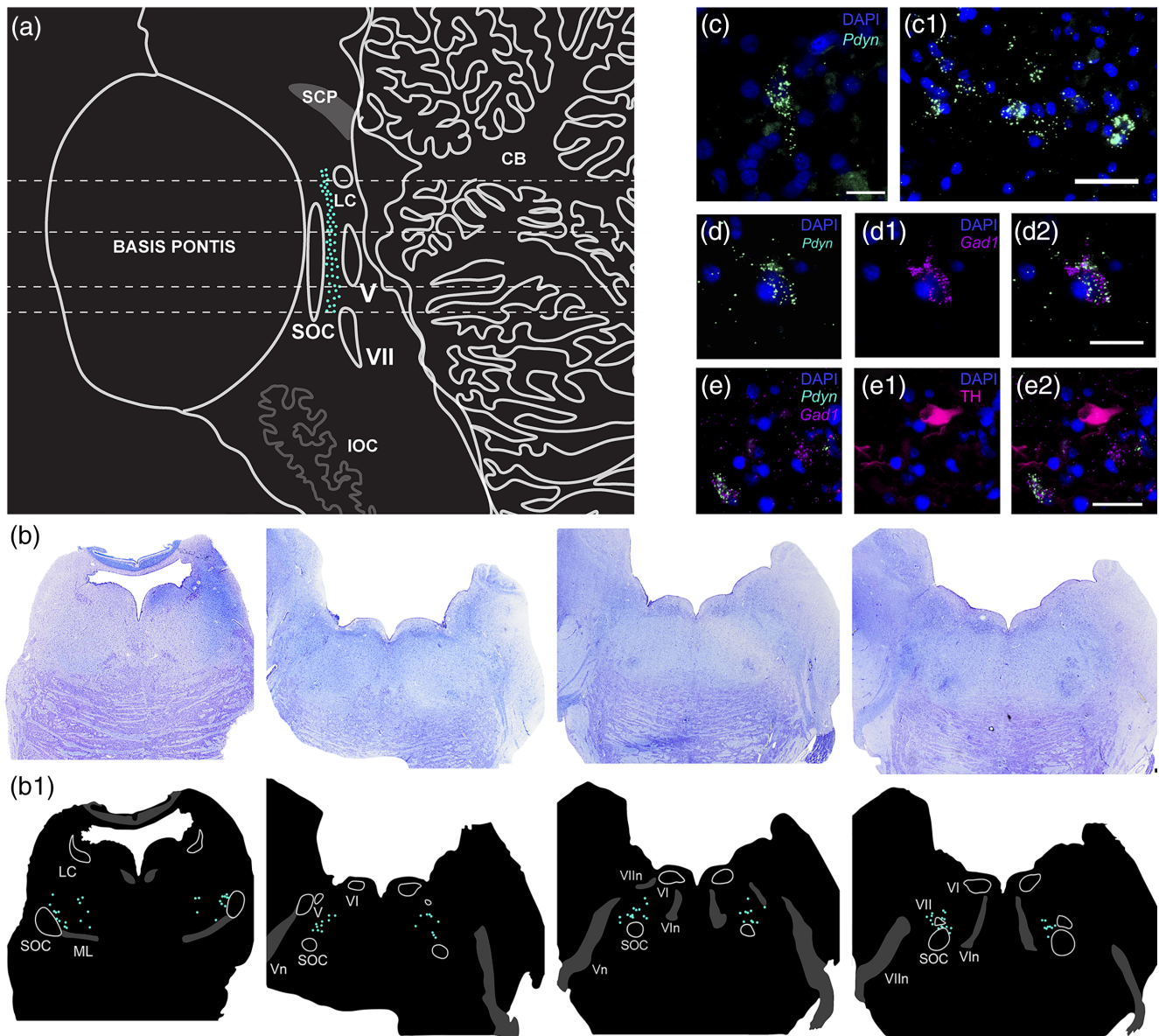
FIGURE 2 LJA5 *Pdyn*-expressing neurons in the human brainstem. (a) Sagittal representation of the LJA5 neurons in a human brainstem. Dotted lines in (a) represent levels of axial sections shown in (b). (b) Nissl-stained axial sections with drawings of adjacent fluorescently labeled sections. Nissl-stained sections of a 35-week gestation female brainstem oriented on the rostral-caudal axis reveal the surrounding neuroanatomical features of the LJA5 region (scale bars are 2 mm). Fluorescent in situ hybridization of brainstem sections revealed a large population of prodynorphin (*Pdyn*)-expressing neurons. These neurons are dorsal to the superior olivary complex (SOC), ventral to the CN VI nucleus, and medial to CN V motor nucleus (moV) and CN VII nuclei and nerves, similar to their location in mice. (c) In situ hybridization revealed a novel group of *Pdyn*-expressing neurons in the human hindbrain. Scale bars are 20 and 50 μm. (d) Colocalization of *Pdyn* (green) and *Gad1* (purple). Scale bar is 20 μm. (e) Immunohistochemistry of the LJA5 region for tyrosine hydroxylase (TH, magenta) shows that the LJA5 neurons are distinct from the A5 adrenergic group. Scale bar is 50 μm [Color figure can be viewed at wileyonlinelibrary.com]

from cervical through sacral spine (Figure 5h–l; Table 2). While projections were often bilateral, innervation was usually densest ipsilaterally.

AAV-DIO-ChR2-mCherry is a membrane bound molecule that robustly labels the entire axon. While this is useful for tracing pathways, it is difficult to distinguish axons of passage from axon terminals. AAV-DIO-synaptophysin-mCherry is a useful indicator as it highlights boutons, emphasizing terminal fields rather than the entire pathway. Therefore, we used mCherry-labeled

synaptophysin to investigate the innervation of target fields. Similar to the injection sites of AAV-DIO-ChR2-mCherry, analysis of AAV-DIO-synaptophysin-mCherry revealed transduction was limited to the LJA5 neurons, a GFP+ cluster of neurons that are immediately rostral to the facial nerve exit (Figure 6). In addition, transduction efficiency was higher with this AAV than with AAV-DIO-ChR2-mCherry, as analysis of AAV-DIO-synaptophysin-mCherry injection sites revealed that 97.9% of LJA5 GFP+ cells expressed mCherry. In contrast
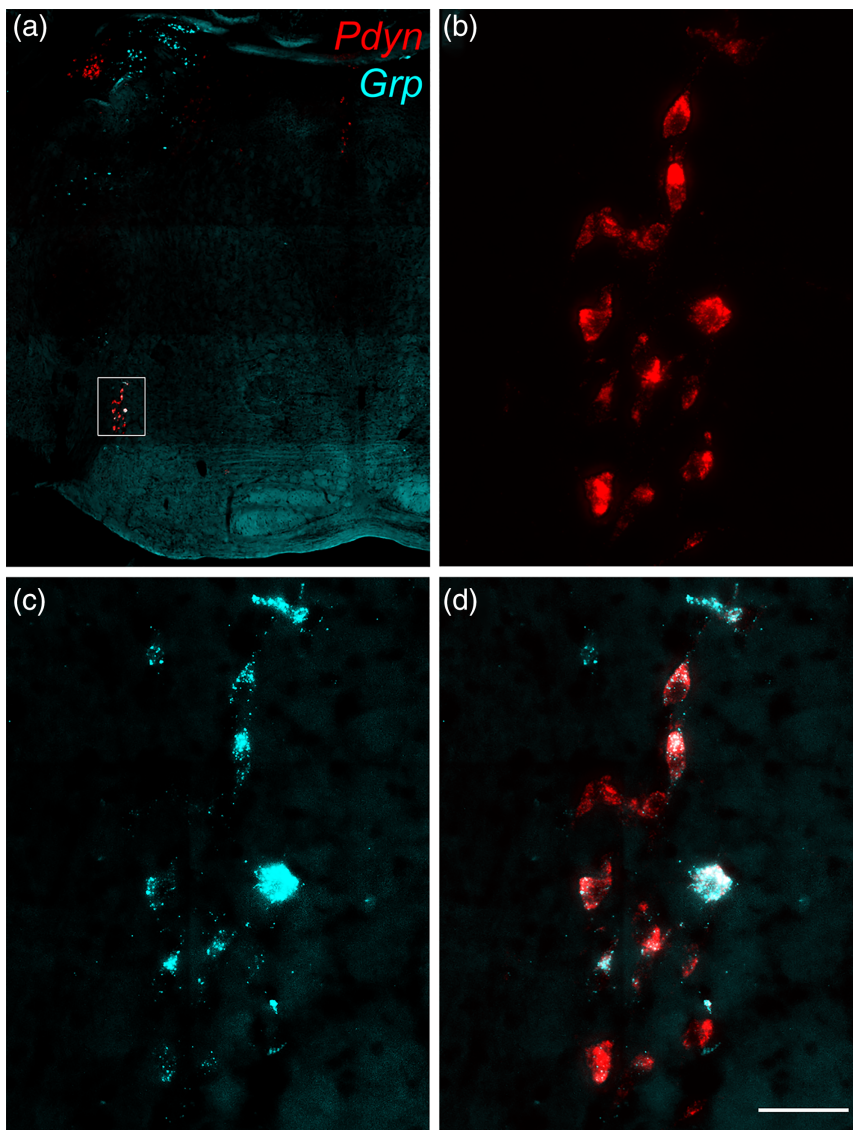
FIGURE 3 LJA5 *Pdyn+* neurons express *Grp*. Coronal section of mouse brain. Within the ventrolateral pons, *Grp* expression (blue) is mostly limited to LJA5 neurons labeled for *Pdyn* (red). Box in (a) is zoomed in for (b)–(d). Scale bar is 50 µm [Color figure can be viewed at wileyonlinelibrary.com]

to ChR2, AAV-DIO-synaptophysin-mCherry had sparse labeling of axons and robustly labeled soma and boutons which highlighted terminal fields.

3.2.1 | PAG

Anterograde tracing with AAV-DIO-ChR2-mCherry revealed dense LJA5 axons and boutons in the PAG. Specifically, innervation was densest in the lateral and ventrolateral PAG (lPAG/vlPAG) rostrally (Figure 5a, b). Caudally, innervation coursed dorsally, following the shifting boundary of the lPAG (Figure 5c). Bouton labeling with AAV-DIO-synaptophysin-mCherry showed a similar pattern of innervation (Figure 7).

In brainstem sections containing the PAG, in situ hybridization identified *Tac1+* neurons, and expression was mainly in the lPAG/vlPAG (Figure 7a). When combined with immunohistochemistry to label synaptophysin mCherry+ LJA5 boutons, we saw mCherry+ boutons clustered among the *Tac1+* PAG neurons (Figure 7). Although we show only one section in this figure, the mCherry boutons

concentrated on *TAC1+* neurons throughout their rostro-caudal extent of the PAG, following the neurons dorsally in caudal sections.

3.2.2 | PB

Our initial tracing experiments with ChR2 revealed abundant LJA5 mCherry+ fibers throughout the LPB, with denser innervation of the dorsolateral subnucleus of the PB (PBdL) (Figure 5d). However, our tracing with synaptophysin labeled fewer axons, revealing that the main terminal field was in PBdL rather than the entire LPB.

We labeled PB sections for genetic markers that subdivide the PB including dynorphin (marked by GFP of our reporter mouse) and FoxP2 (Figure 8), which mark thermosensory relay neurons (Geerling et al., 2016). We analyzed three levels of the PB: Rostral at the level of the rostral-to-external lateral subnucleus (PBreL, Figure 8a) marked predominately by FoxP2+ neurons and sparse dynorphin (GFP); the central lateral subnucleus (PBcL, Figure 8b) where FoxP2+ neurons extend dorsally to densely clustered GFP+ neurons; and

FIGURE 4 Injection site of AAV-DIO-ChR2-mCherry (anterograde tracer) into LJA5 neurons. LJA5 dynorphinergic neurons (GFP) are transduced with AAV-DIO-ChR2-mCherry (red). Scale bar is 50 μm [Color figure can be viewed at wileyonlinelibrary.com]
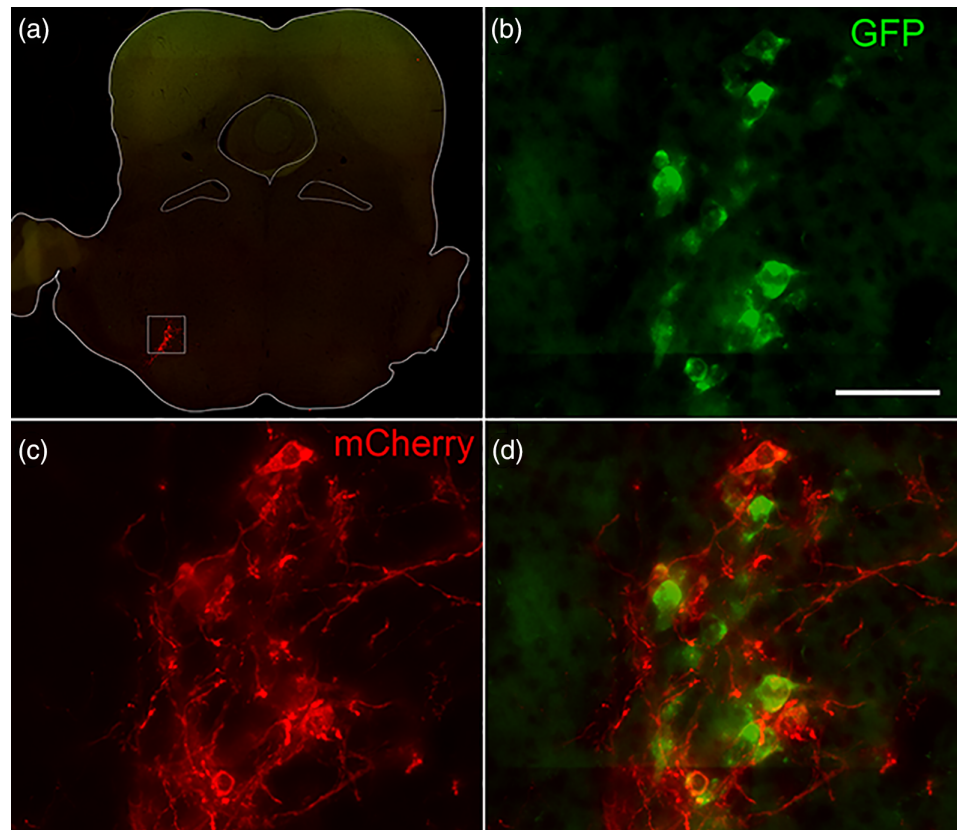
caudally at the dorsal lateral subnucleus (PBdL, Figure 8c) where FoxP2 is clustered among the GFP+ neurons. At each level, we saw mCherry+ fibers clustered in the dorsolateral PB, with boutons densest both dorsal and lateral to the FoxP2+ and GFP+ neurons (Figure 8d). The LJA5 fibers largely avoided the external lateral subdivision of the parabrachial (PBeL) as marked by *Tac1*+ neurons (Figure 9), which are known to promote nocifensive behaviours (Barik, Thompson, Seltzer, Ghitani, & Chesler, 2018), and the medial parabrachial nucleus (MPB).

3.2.3 | Medulla

Caudal to the facial nerve exit, LJA5 axons coursed ventrolaterally and then dorsomedially toward the NTS. Fibers crossed through dorsal motor nucleus of vagus, terminating in the ventrolateral nucleus of the solitary tract (NTS) (Figure 5e).

In the medulla, ChR2 mCherry+ fibers are sprinkled around the ventrolateral medulla, just medial to the ventromedial edge of the spinal trigeminal nucleus (Figure 5e,f). Labeling was densest caudally, just anterior to and at the level of the pyramid decussation (Figure 5f), a region referred to as the caudal pressor area (CPA) (Gordon & McCann, 1988; Sun & Panneton, 2002).

In cases traced with synaptophysin-mCherry, we labeled medullary sections for mCherry and tyrosine hydroxylase (TH). In the caudal medulla, the A1 noradrenergic cell group is marked by TH, which is just medial to the CPA. While some mCherry+ boutons opposed TH+

soma in the A1 noradrenergic cell group, mCherry+ boutons most densely innervated the region just lateral to the A1 soma in the CPA, which contains some TH+ proximal axons (Figure 10).

Innervation was densest through the superficial layers (lamina I) of the spinal trigeminal nucleus (Figure 5g), a region continuous with lamina I of the spinal cord.

3.2.4 | Spinal cord

Continuous with projections in the spinal trigeminal nucleus, LJA5 axons and boutons specifically targeted lamina I, from cervical to sacral spinal levels (Figure 5h–l). Outside of lamina I, the only substantial labeling in the spinal cord was ventral to lamina I in the lateral spinal nucleus (LSN).

In cases traced with synaptophysin-mCherry, we labeled spinal sections for mCherry along with dynorphin (GFP), and *Tac1* which are found in lamina I (Figure 11). mCherry terminals appeared to make close appositions with superficial dynorphin (GFP+) neurons while axons largely remained superficial to the *Tac1*+ neurons.

3.3 | LJA5 afferent projections

Two cases had CTb injections that encompassed almost all of the GFP+ LJA5 neurons without extension into the SOC (Figure 12). We
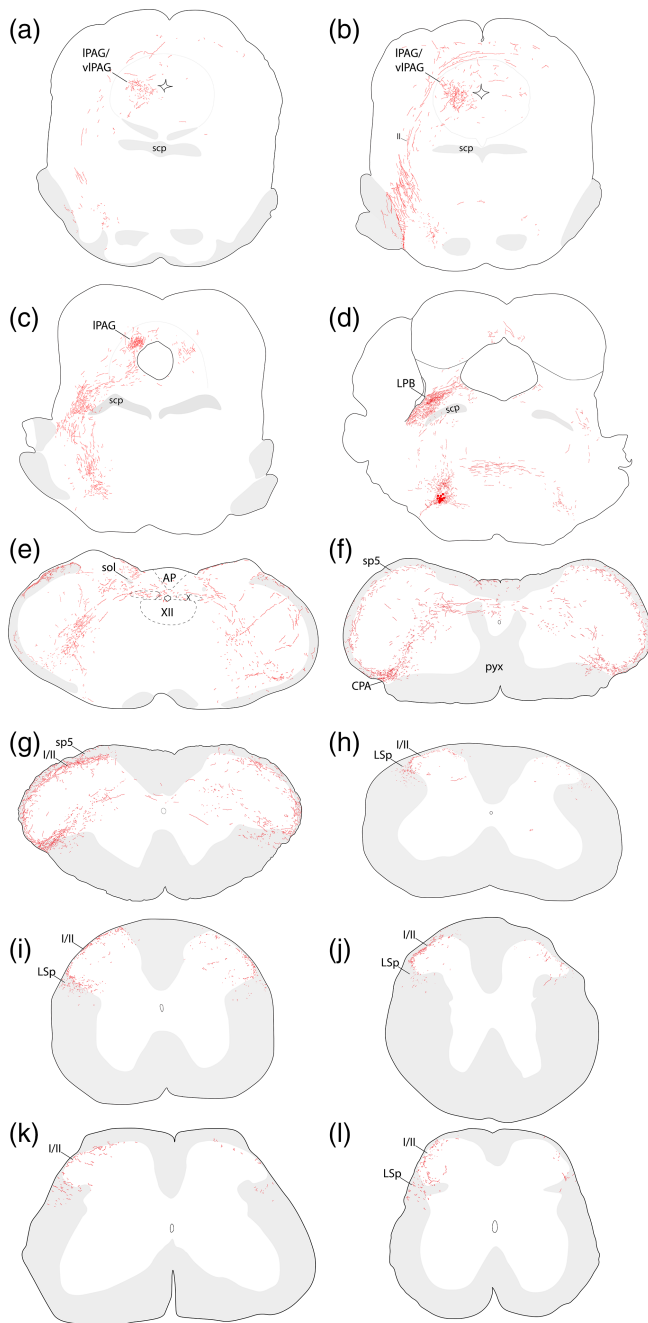
FIGURE 5 Anterograde tracing from LJA5 neurons. Red circles in D indicate a representative injection site of AAV-DIO-ChR2-mCHerry into LJA5 neurons. Red lines indicate axons and boutons originating from the LJA5 neurons [Color figure can be viewed at wileyonlinelibrary.com]

analyzed retrograde labeling in these brains (Table 2), and the inputs are illustrated in one case (Figure 13).

Retrogradely labeled cells were found in a specific pattern through the entire rostrocaudal extent of the cortex (Figure 13). Rostrally, cells were clustered in the cingulate cortex that trickled ventrally into infralimbic cortex (Figure 13a,b). Caudally, labeled cells remained in this dorsal medial portion of cortex around the truncal region of somatosensory cortex (Figure 13e–g). Strikingly,

there was a more densely clustered group of labeled cells ventrolaterally in layer 5 of the somatosensory/insular junction which extended through the entire rostro-caudal extent of the cortex (Figure 13d–h).

Among subcortical forebrain areas, the lateral preoptic area, ventrolateral divisions of the bed nucleus of the stria terminalis (BNST), paraventricular hypothalamus (PVH), central nucleus of the amygdala (CEA), lateral hypothalamus (LHA), and dorsomedial hypothalamus (DMH) were moderately labeled, and parasubthalamic nucleus was densely labeled (Figure 13d–g).

Within the midbrain, the PAG was heavily labeled, with the LPAG containing the most labeled cells (Figure 13h–j), similar to the distribution of anterogradely labeled LJA5 fibers.

Within the pons, the densest labeling was in the LPB, especially the PBdl (Figure 13k). Retrogradely labeled neurons were uncommon in the MPB. Additionally, there were many retrogradely labeled neurons in the contralateral LJA5 region (Figure 13k).

In the medulla, there were moderate CTb + neurons in the reticular formation, NTS, and a cluster in the lateral reticular nucleus (Figure 13l). Caudally, there was moderate labeling in the CPA at the level of the pyramid decussation (Figure 13m). Retrogradely labeled neurons were sparse caudal to the pyramidal decussation, although there were a few in the spinal trigeminal tract and nucleus (Figure 13n).

4 | DISCUSSION

We identified a group of brainstem neurons with a sensory region-specific projection pattern, which we named LJA5. Here, we characterize LJA5 neurons in mouse and human brains and provide a detailed analysis of the mouse efferent and afferent projections through the entire brain and spinal cord, including markers of cell types within the LJA5 target regions.

LJA5 neurons express *Pdyn*, the gene for prodynorphin, the precursor protein for the inhibitory opioid neuropeptide dynorphin. Previous studies characterizing *Pdyn* expression and dynorphin distribution throughout the rat brain have failed to comment on these ventral brainstem neurons (LJA5), although a few prodynorphin/dynorphin expressing neurons can be seen around the facial nerve in previously published figures (Fallon & Leslie, 1986; Merchenthaler et al., 1997). Importantly, LJA5 *Pdyn+* neurons are GABAergic as they express *Gad1*, and we predict that LJA5 neurons inhibit their targets.

Dynorphin primarily binds to the kappa opioid receptor, which is expressed by neurons in many brain and spinal regions, including lamina I of the spinal cord (Harris, Chang, & Drake, 2004; Waldhoer et al., 2004). Kappa opioid agonists have been shown to be analgesic (Ansonoff et al., 2006; Kivell & Prisinzano, 2010) and antipruritic (Inan & Cowan, 2004; Kardon et al., 2014; Kumagai et al., 2012; Wikstrom et al., 2005) in mice and humans. Our discovery of dynorphinergic, lamina I-projecting neurons suggests an endogenous source of dynorphin for kappa-opioid inhibition of pain and itch sensory transmission.

Interestingly, we found that most LJA5 *Pdyn+* neurons also express *Grp*, but there are a few small *Grp+* neurons intermingled that
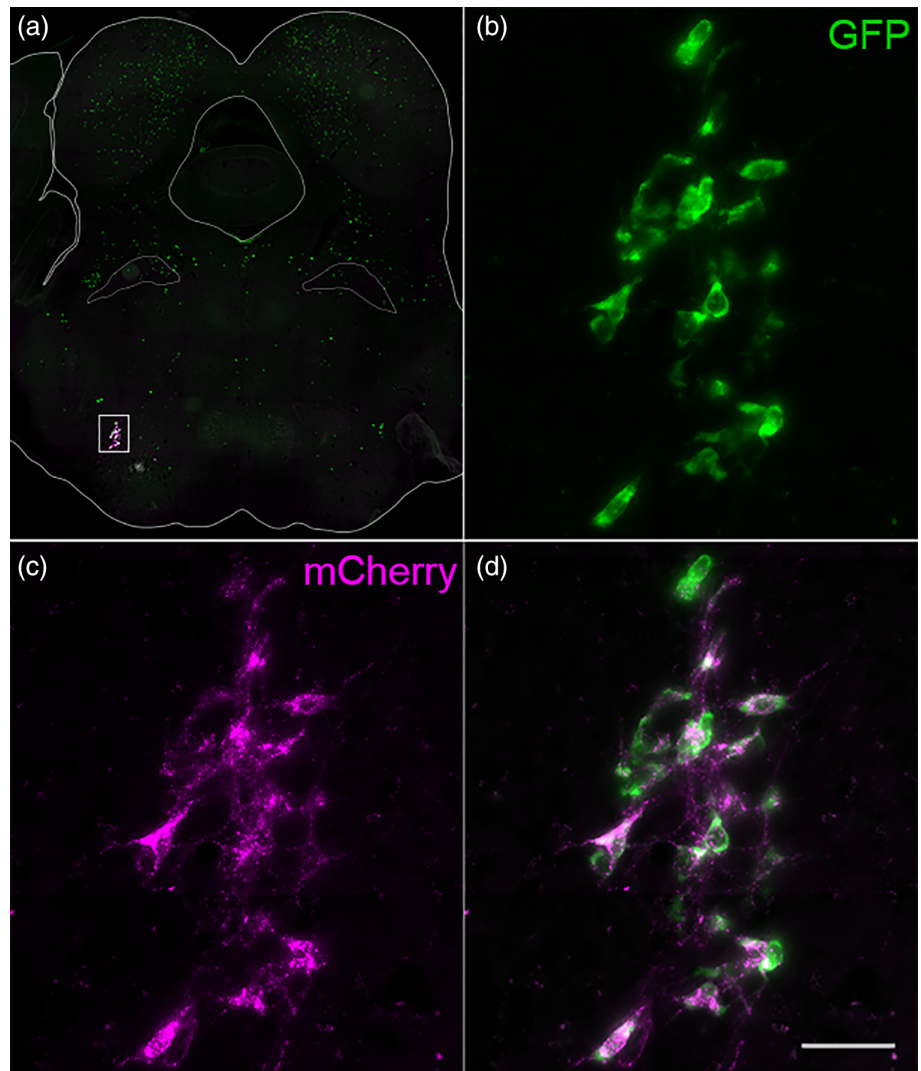
do not express *Pdyn*. We do not know if these smaller *Grp+/Pdyn*- neurons also project to lamina I and PB, or if they are a separate population of neurons with distinct projections and functions. GRP binds to GRP receptors (GRPR), and GRPRs signal through a Gq cascade (Roesler & Schwartsmann, 2012), indicating that GRP predominately has an excitatory effect on its targets. *Grp* is more highly expressed in the forebrain, but it is also seen in the brainstem including the parabrachial nucleus (Wada, Way, Lebacq-Verheyden, & Battey, 1990). A study analyzing the distribution of *Grp* neurons commented on a small cluster of neurons in the principle sensory nucleus of the trigeminal (PrV), but this is likely to be the LJA5 *Pdyn+* neurons that are just ventral to PrV (Wada et al., 1990).

4.1 | LJA5 in human brain

LJA5 *Pdyn*-expressing neurons are located in similar parts of the human brainstem as in the mouse. A large population of neurons expressing prodynorphin are identified in the rostral, ventrolateral

hindbrain. In humans, this cell group spans from the PB to CN VII, analogous to the pattern in mouse brainstem. The LJA5 neurons are located next to the facial nerve exit, close to the region that contains the A5 adrenergic cell group (Saper & Petito, 1982). As in mouse, the LJA5 *Pdyn+* neurons are distinct from the TH+ A5 neurons, and they are GABAergic (express *Gad1*).

A prior analysis of dynorphin proteins in the human brainstem was limited to an immunohistochemical study of the parabrachial area with no mention of dynorphin in other parts of the brainstem (Fodor et al., 1992). Additionally, as in our experience, immunohistochemistry for the dynorphin protein is not sensitive enough to detect most *Pdyn+* soma due to trafficking of protein away from the cell body. To address this, we instead utilized a fluorescent in situ hybridization approach to visualize *Pdyn* mRNA levels in human brainstem tissue. This strategy revealed the novel population of LJA5 neurons spanning throughout the pons.

There are reports of strokes in the lateral medulla (Wallenberg syndrome) and lateral pons causing neuropathic itch (Fitzek et al., 2006; Oaklander, 2012), and pain associated with onset of these
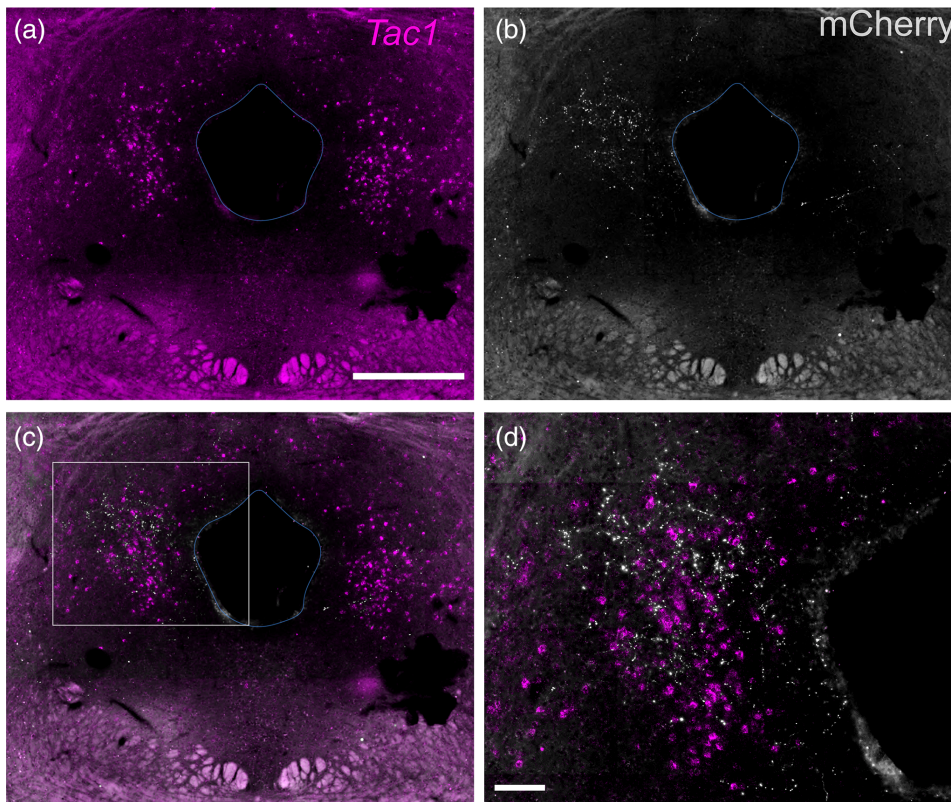
FIGURE 7 LJA5 axons project to lateral periaqueductal gray (a)–(c). AAV-DIO-synaptophysin-mCherry injection into LJA5 of a *Pdyn*-GFP mouse shows that mCherry+ terminal axons and boutons (white) project to the lateral PAG, in the region that is *Tac1*+ (magenta). Scale bar is 500 μm in (a) and 100 μm in (d) [Color figure can be viewed at wileyonlinelibrary.com]
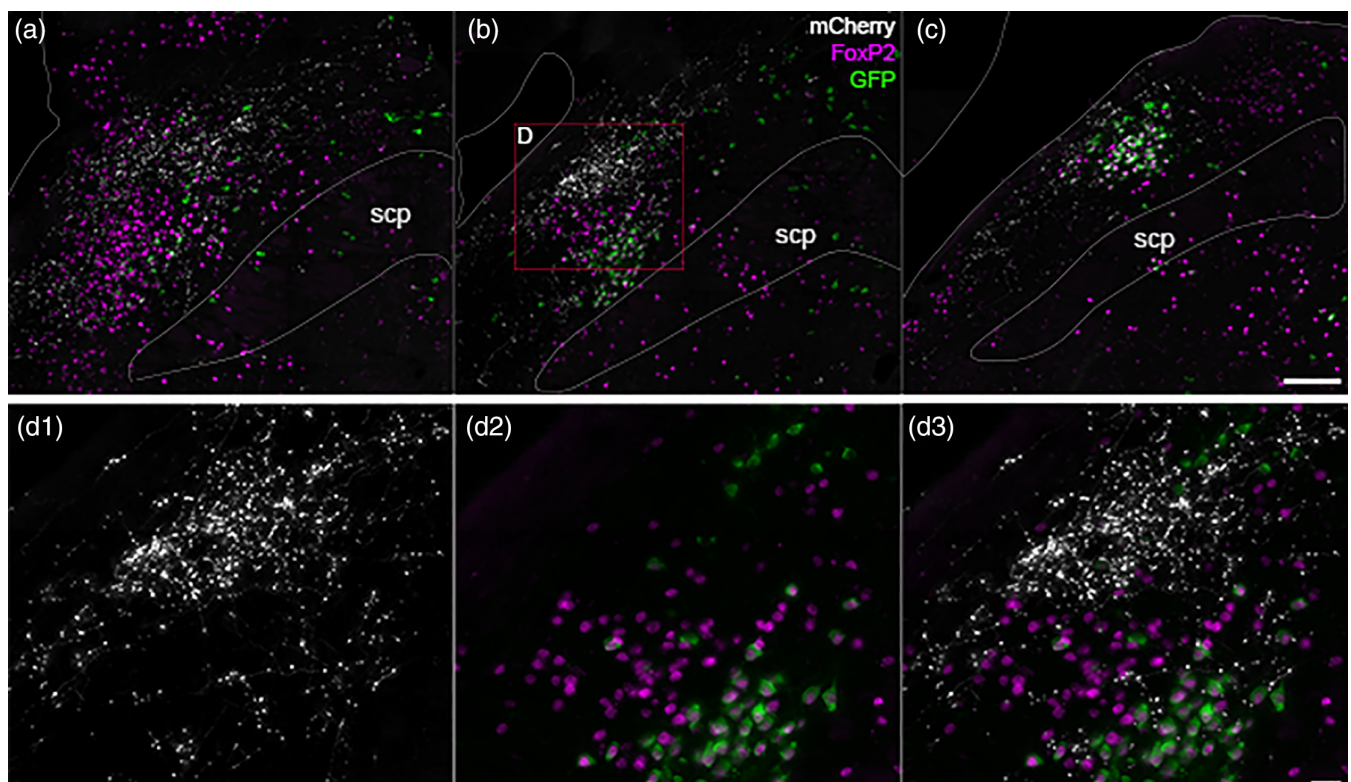

FIGURE 8 LJA5 axons project to lateral parabrachial nucleus. (a)–(c) AAV-DIO-synaptophysin-mCherry injection into LJA5 of a *Pdyn*-GFP mouse shows that mCherry+ terminal axons and boutons (white) project to the lateral parabrachial nucleus, but avoid the region that is heavy in FoxP2 (purple) labeling or dynorphin (GFP) (scalebar is 200 μm in [c] and 50 μm in [d]). Red box in (b) demonstrates the zoomed area shown in d1-3 [Color figure can be viewed at wileyonlinelibrary.com]

FIGURE 9 LJA5 axons project to the dorsolateral PB. AAV-DIO-synaptophysin-mCherry injection into LJA5 of a *Pdyn*-GFP mouse shows that mCherry+ terminal axons and boutons (white) project to LPB and are concentrated dorsal to the *Tac1*+ neurons of the PBel (magenta) and the dynorphin neurons in the PBcl (GFP). Scale bar is 100 μm [Color figure can be viewed at wileyonlinelibrary.com]
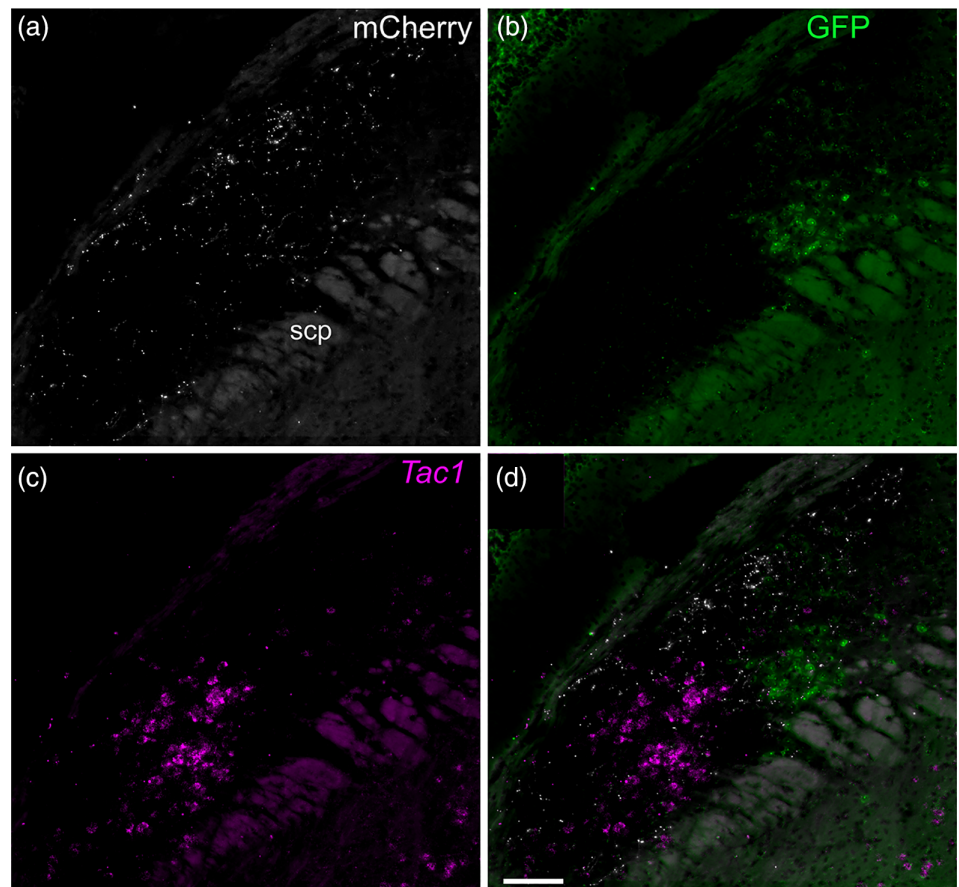
strokes (Fitzek et al., 2006). Perhaps the pruritis and pain in these patients is due to lesions of LJA5 inhibitory neurons.

4.2 | Comparison with previous literature

While LJA5 neurons have not been discussed in previous literature, they are located adjacent to the more well-known catecholamine group, A5, and therefore may have been incidentally included in prior studies. Early A5 tracing studies used conventional tracers which lack genetic specificity, so they trace from any neuron that they come in contact with. Considering that LJA5 neurons are adjacent to A5 neurons, it is possible that previous A5 tracing studies have included projections from LJA5 neurons. Previous tracing studies show that A5 efferents are largely distinct from LJA5 neurons including many forebrain structures and intermediolateral (IML) cell column where we do not see labeling (Byrum & Guyenet, 1987; Clark & Proudfit, 1993). However, both A5 and LJA5 appear to innervate the PAG, LPB, caudal pressor area, and LSN, but as conventional tracers lack genetic specificity, some of these apparent A5 projections may actually arise from the LJA5 neurons.

A later study using conditional tracing confirmed the A5 spinal projections to thoracic IML, and in particular to the sympathetic pre-ganglionic neurons (Bruinstroop et al., 2012). Additionally, this study showed that the A5 dorsal horn and LSN projections were more sparse than the previous conventional tracing study suggested

(Bruinstroop et al., 2012). Therefore, it is likely that projections from the LJA5 neurons underlie the LSN and lamina I labeling seen by Clark and Proudfit.

We report that LJA5 neurons project to many areas known to mediate sensory functions. Here, we place these findings in the context of existing data and discuss the functional implications of LJA5 neurons with their efferent and afferent connections.

4.3 | Periaqueductal Gray

The idea that the PAG could produce analgesia began with an observation in 1969 when electrical stimulation at the edge of the PAG allowed scientists to operate on rats without anesthesia (Reynolds, 1969). Since then, studies on the descending control of pain have focused on the PAG projection to the rostral ventromedial medulla (RVM), which projects nonspecifically across the spinal cord (Fields, Heinricher, & Mason, 1991; Millan, 2002). Additionally, there are direct projections from lamina I of the spinal cord to the PAG (Bernard, Dallel, Raboisson, Villanueva, & Le Bars, 1995), implicating the PAG in both nociceptive reception and descending modulation.

Within the PAG, most of the RVM-projecting neurons are located in the lPAG/vlPAG, and many of these projection neurons contain substance P (SP) (Yin et al., 2014). These SP+ neurons follow a ventral to dorsal shift through the rostro-caudal extent of the PAG (Moss &
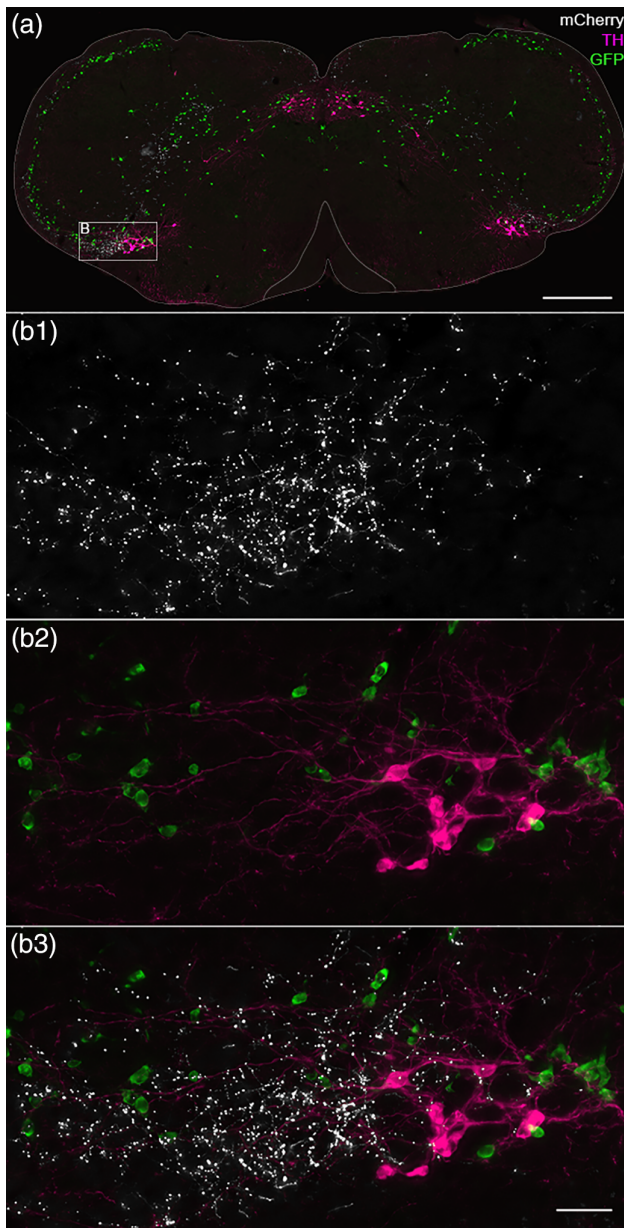
FIGURE 10 LJA5 axons innervate the caudal pressor area in the medulla. (a) AAV-DIO-synaptophysin-mCherry injection into LJA5 of a *Pdyn*-GFP mouse shows that mCherry+ terminal axons and boutons (white) project to the caudal pressor area, lateral to TH+ A1 neurons (pink). Box in (a) is zoomed in for (b). (Scalebar is 500 μm in [a] and 50 μm in [b]) [Color figure can be viewed at wileyonlinelibrary.com]

Basbaum, 1983), much like the input pattern we see from LJA5 fibers that travel dorsally (Figure 5a–c). SP is made from the gene *Tac1*. A recent study showed that *Tac1+* PAG neurons are more active during itch-induced scratching, and lesioning or silencing these neurons reduces itch-induced scratching (Gao et al., 2019). Additionally, activation of these neurons induced spontaneous scratching. We found that LJA5 neurons innervate lPAG and vlPAG *Tac1+* neurons (Figure 7), following their ventral to dorsal shift along the rostrocaudal trajectory. Considering the inhibitory nature of the LJA5 neurons, LJA5 innervation of *Tac1+* PAG neurons might be an antipruritic mechanism.

Additionally, we find that the lPAG innervates the LJA5 region, implying reciprocal connections between these two areas. A previous anterograde tracing study from the lateral PAG show dense innervation of "the A5 region" which might also represent the LJA5 neurons (Cameron, Khan, Westlund, & Willis, 1995).

The PAG has mixed effects on pain and itch sensation. PAG stimulation induces analgesia (Liebeskind, Guilbaud, Besson, & Oliveras, 1973; Yeung, Yaksh, & Rudy, 1977). In contrast, PAG stimulation increases scratching behavior while PAG inhibition reduces scratching in mice (Gao et al., 2019). Given this heterogeneity among PAG neurons in regards to nociception (Samineni et al., 2017), further studies are required to clarify the functional relationship between LJA5 and PAG neurons.

4.4 | Parabrachial nucleus

Few prior studies have investigated the afferent projections of the parabrachial nucleus (PB). Previous studies focused on the forebrain afferents, stopping analysis just rostral to sections that would contain LJA5 neurons (Moga et al., 1990), or their analysis skipped over brainstem sections that would contain LJA5 neurons (Tokita, Inoue, & Boughter Jr., 2009). Therefore, we do not know of existing literature describing the projection from the LJA5 region to the LPB, and ours is likely the first description of connectivity between the two regions.

Traditionally, sensory information (pain, itch, and temperature) was thought to be transmitted from the periphery to the brain via the spinothalamic pathway. However, multiple studies have shown that lamina I neurons of the spinal cord directly project to the PB (Bernard et al., 1995; Cechetto, Standaert, & Saper, 1985; Craig, 1995; Panneton & Burton, 1985), comprising the spinoparabrachial pathway. In fact, over 80% of lamina I neurons that project to the thalamus also send collaterals to the parabrachial nucleus (Hylden, Anton, & Nahin, 1989).

Lamina I projection neurons of the spinal cord directly innervate many subdivisions of the PB, including PBdL, lateral crescent, and superior lateral subnuclei (Bernard et al., 1995; Cechetto et al., 1985). Furthermore, electrophysiology studies confirmed connectivity between nociception-specific lamina I neurons and PB neurons (Bester, Chapman, Besson, & Bernard, 2000; Light, Sedivec, Casale, & Jones, 1993), and ablation of the LPB is antinociceptive (Rodriguez et al., 2017) and antipruritic (Mu et al., 2017). The lamina I innervation of the PBdL appears similar to the distribution of LJA5+ fibers, suggesting that LJA5 terminals may inhibit ascending nociceptive information relayed from the spinal cord to the LPB.

The neurochemical identity of the LPB neurons innervated by LJA5 fibers remains unknown. However, we wanted to assess if LJA5 neurons innervate LPB neurons that mediate temperature, itch and pain behaviors. Within the LPB, LJA5 mCherry+ terminals mostly innervate neurons dorsal to FoxP2+ and prodynorphin (GFP+) neurons (Figure 8) which have been shown to be thermosensory relay neurons (Geerling et al., 2016). Therefore, it is less likely that LJA5 affect PB-mediated thermosensation. *Tac1+* LPB neurons promote
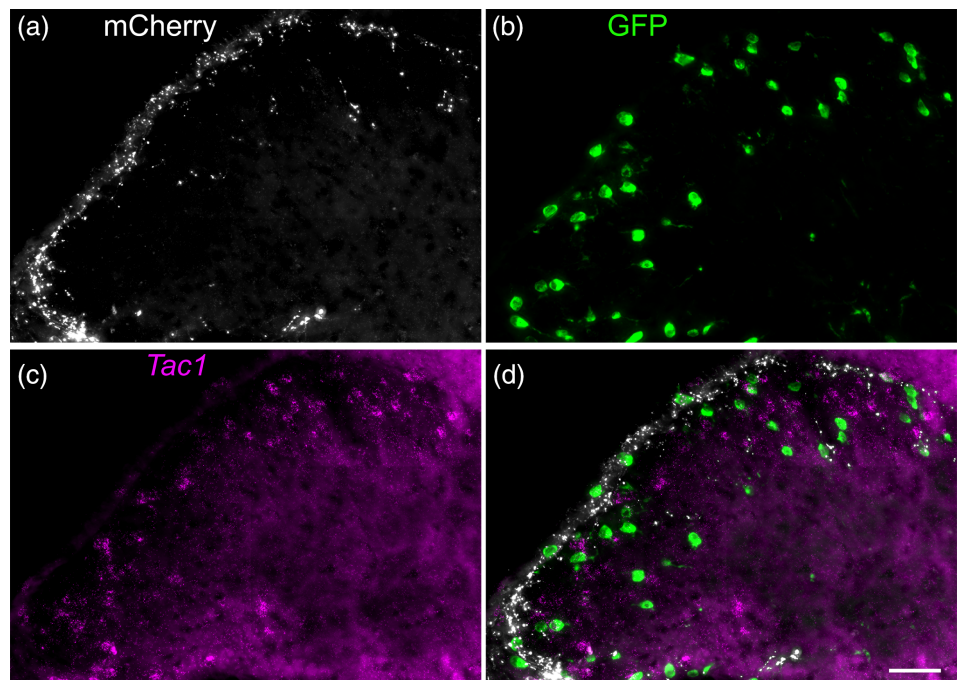
nocifensive behaviors such as jumping/escape behavior in response to heat, and licking behavior in response to formalin induced pain (Barik et al., 2018). Calcitonin gene-related peptide-expressing neurons (CGRP) respond to pain (Campos, Bowen, Roman, & Palmiter, 2018), and ablation is antinociceptive (Han, Soleiman, Soden, Zweifel, & Palmiter, 2015) and antipruritic (Campos et al., 2018). *Tac1*+ LPB neurons are located ventrolaterally to *Pdyn*+ neurons in the external lateral subdivision of the parabrachial (PBel), and some of the ventral *Tac1*+ neurons also express *calca1*, the gene for CGRP(Barik et al., 2018). LJA5 fibers largely avoid the PBel, as marked by the *Tac1* + neurons (Figure 9) and CGRP. Therefore, we do not currently have a marker for the LPB region innervated by LJA5 fibers.

Lastly, after injection of CTb in the LJA5 region, LPB neurons were densely labeled, especially the PBdl (Figure 13k). This pattern is similar to the location of anterogradely labeled LJA5 fibers, implying that these PB neurons may be reciprocally connected to LJA5 neurons.

4.5 | Caudal pressor area

The LJA5 neurons densely innervate a region just lateral to the A1 neurons, known as the caudal pressor area (CPA) (Figures 5f and 9). The caudal pressor area is located just dorsal to the lateral reticular nucleus at the level of the pyramid decussation and the caudal edge of the inferior olives (Gordon & McCann, 1988), and just lateral to A1 (Sun & Panneton, 2002). The CPA was functionally defined as a region where stimulation increases blood pressure (Gordon & McCann, 1988; Sun & Panneton, 2002).

The CPA innervates many sensory regions, including the A5 region (Sun & Panneton, 2005) which appears as dense innervation

just medial to the facial nerve exit. While this study does not show sections immediately rostral to this level of the facial nerve, these CPA fibers might actually be projections to LJA5, reciprocal connections to the LJA5 neurons which we also saw with our retrograde tracing (Figure 13m). Given that blood pressure tends to increase with pain (Fagius, Karhuvaara, & Sundlof, 1989; Maixner, Gracely, Zuniga, Humphrey, & Bloodworth, 1990; Nordin & Fagius, 1995), it is possible that LJA5 neurons can inhibit both noxious sensations and the accompanying rise in blood pressure via projections to the CPA.

4.6 | Spinal cord

Perhaps the most remarkable feature of LJA5 neurons is that they are the only group of inhibitory neurons known to directly and selectively innervate lamina I of the spinal cord, which relays all pain, itch, and thermal sensory information from the skin to the brain. LJA5 neurons closely appose dynorphin neurons in lamina I which project to the PB (Standaert, Watson, Houghten, & Saper, 1986) implying that LJA5 neurons might be inhibiting the connection of sensory information from the spinal cord to the brain.

Additionally, we saw a very similar pattern of lamina I innervation in the most superficial spinal trigeminal nucleus, which supplies sensory information (itch, pain and temperature) to the face. This area can be considered a medullary extension of lamina I, and it also innervates the parabrachial nucleus like lamina I of the spinal cord (Cechetto et al., 1985). Therefore, we predict that LJA5 neurons inhibit cutaneous sensation in the face, in addition to body.

Outside lamina I, the only substantial LJA5 terminals we find in the spinal cord target the adjoining lateral spinal nucleus (LSN), a loose collection of neurons in the dorsolateral funiculus. LSN
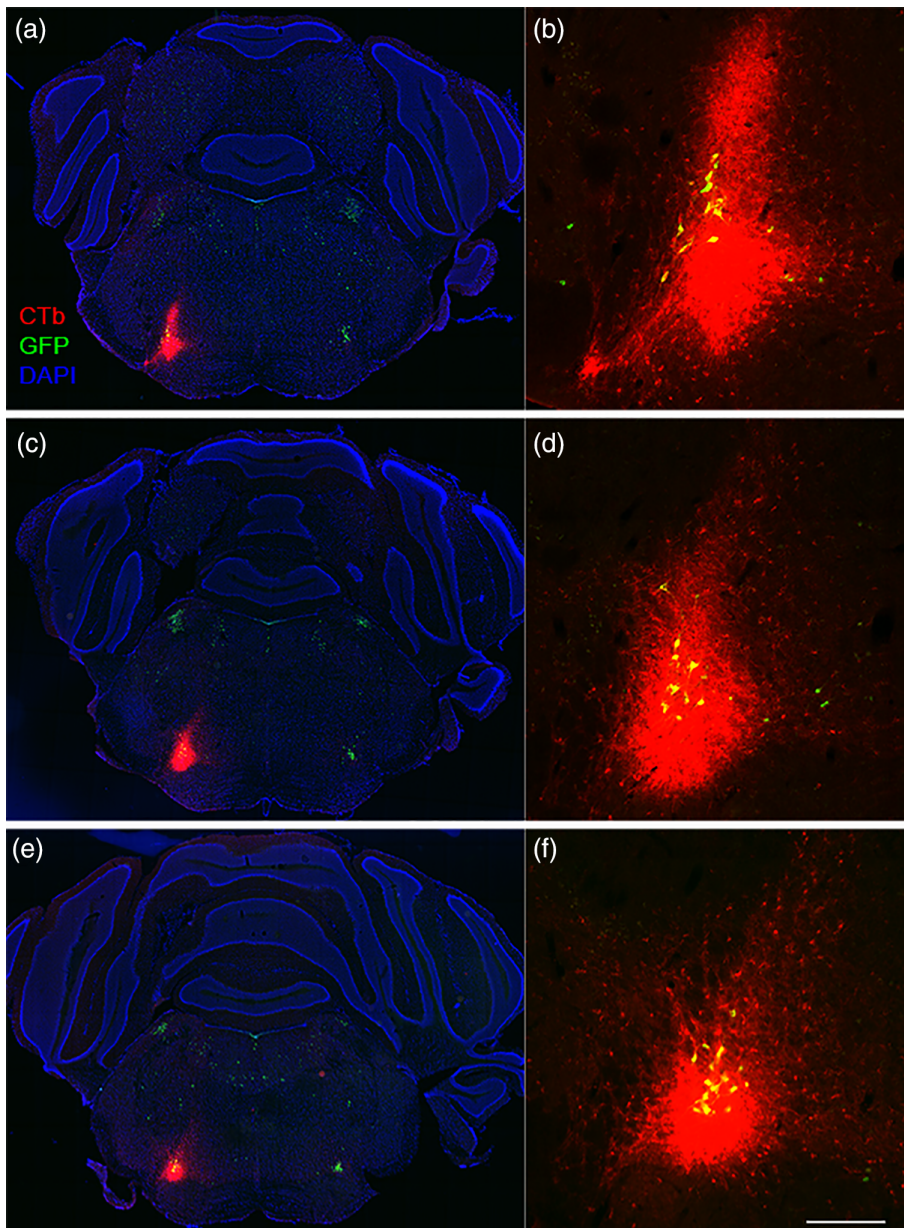
FIGURE 12 Injection site of CTb (retrograde tracer) into LJA5 neurons. Right panels are zoomed in from left panels. Scale bar is 200 μm [Color figure can be viewed at wileyonlinelibrary.com]

neurons receive nociceptive signals via polysynaptic inputs and primary afferents, similar to lamina I, but from subcutaneous and visceral tissues (Neuhuber, 1982; Neuhuber & Sandoz, 1986; Sikandar, West, McMahon, Bennett, & Dickenson, 2017). Thus, LJA5 projections to the spinal cord are well positioned to inhibit the full suite of noxious sensory information transmitted through the spinal cord to the brain.

We showed that LJA5 *Pdyn+* neurons also express *Grp*, and GRP binds to GRPR. In the spinal cord, *Grp* is limited to lamina I (Sun & Chen, 2007; Sun et al., 2009) indicating that LJA5 neurons which selectively project to lamina I might have an influence on these *Grpr+* lamina I neurons. Deletion of *Grpr or Grpr+* neurons in the spinal cord results in itching defects, while sparing pain responses (Sun & Chen, 2007; Sun et al., 2009). Therefore, LJA5 activation might mediate itch sensation via *Grpr+* lamina I neurons, but the role of GRP,

dynorphin, and GABA transmission from LJA5 neurons within lamina I needs to be distinguished.

Additionally, *Tac1+* neurons in lamina I project to LPB, and ablation of these lamina I neurons produces indifference to sustained pain but acute, reflex nocifensive behaviors were intact (Huang et al., 2019). LJA5 fibers were largely superficial to these *Tac1+* lamina I neurons.

4.7 | Forebrain

The LJA5 neurons do not innervate the forebrain (the most rostral structure innervated was the PAG), but they receive many inputs from the forebrain. One of the most interesting findings was the input from layer 5 of the somatosensory and insular cortex (Figure 13c-h), which
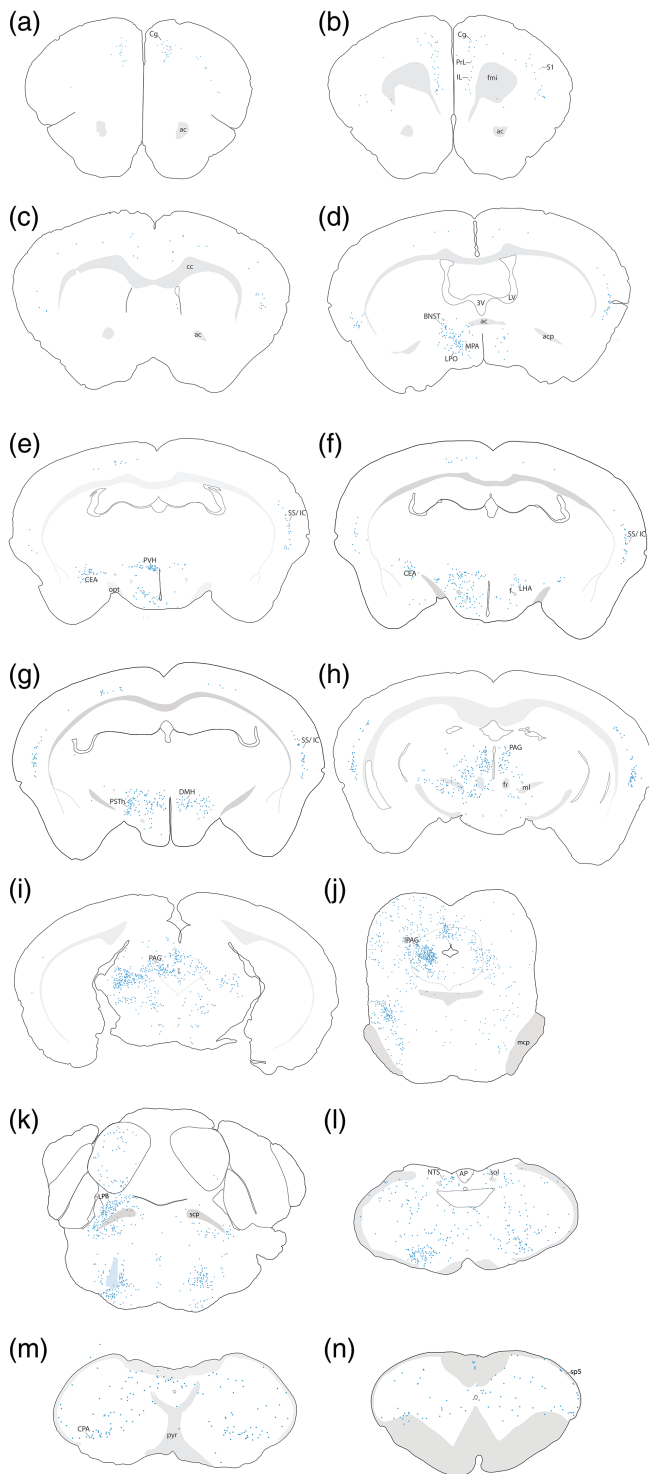
FIGURE 13 Retrograde tracing from LJA5 neurons. CTb injection site at LJA5 neurons (k) is represented by light blue region in lower left pons. Blue dots mark retrogradely labeled neurons [Color figure can be viewed at wileyonlinelibrary.com]

contains brainstem and amygdalar projection neurons (Kapp, Schwaber, & Driscoll, 1985). The insula has been implicated in interoceptive functions (subjective feelings from the body) such as pain, itch, temperature, thirst, hunger, nausea, etc. (Craig, 2009; Gogolla, 2017).

These cortical sensory/interoceptive neurons might first provide important sensory information to an animal to influence behavior accordingly, and perhaps this cortical projection activates LJA5 neurons which then appropriately dampen excessive noxious sensation.

Additionally, we saw dense input from regions that are active during stress such as the preoptic area, BNST, central amygdala, PVH, and DMH. It is known that cortical and amygdalar regions project to BNST, DMH, and POA, which in turn project to PVH to drive the glucocorticoid responses (Jankord & Herman, 2008). This suggests that LJA5 neurons might be activated by stress (by many of the regions that provide input to, and including, the PVH), and LJA5 neurons would then in turn inhibit pain and itch. Stress or fear can be acutely analgesic (Akil, Mayer, & Liebeskind, 1976; Madden, Akil, Patrick, & Barchas, 1977), perhaps so an animal can focus on behavioral responses without much distraction from pain or itch (Amit & Galina, 1988). Interestingly, stress-induced analgesia (SIA) can be blocked by lesions to the central nucleus of the amygdala, an input to LJA5 region (Figure 13e,f) (Helmstetter & Bellgowan, 1993; Ortiz, Close, Heinricher, & Selden, 2008; Veinante, Yalcin, & Barrot, 2013). Considering the adaptive role of stress-induced analgesia, it would make sense that there would be one circuit that receives input about the stressful situation and directly inhibits distracting sensations, and LJA5 neurons might are well positioned for this.

5 | LIMITATIONS

CTb is a conventional, protein tracer that traces from any cell type within the region it is injected. Therefore, the retrogradely labeled inputs are to the LJA5 region, but are not specific to LJA5 neurons. Therefore, we compared our list of inputs with prior studies injecting adjacent regions to see which inputs might be common among injections more centered over adjacent nuclei such as A5 of SOC. However, to really know which of these inputs are specific to LJA5 neurons, we would need to conduct rigorous electrophysiology studies demonstrating synaptic connectivity.

Additionally, our Cre-reporter mice enable easy identification of *Pdyn+* neurons, but Cre-reporter mice can "over-report" as they will express GFP in neurons into adulthood even if neurons only transiently expressed *Pdyn* during development (Geerling et al., 2016). Therefore, not all neurons that express GFP may produce dynorphin in adulthood. However, we have mitigated this concern by testing many of our reporter mice with *Pdyn* in situ hybridization, and in the LJA5 area, all of the clustered GFP+ magnocellular neurons contained *Pdyn*, and only small GFP neurons in the periphery were *Pdyn*-. Additionally, all of the *Pdyn+* neurons in this area contained GFP, suggesting that these Cre-reporter mice are not under-reporting.

6 | CONCLUSION

We describe a novel group of *Pdyn*-expressing neurons in the ventrolateral pons of the mouse and human. This is the first description of

neurons sending direct inhibitory projections specifically targeting lamina I of the spinal cord. This finding, along with projections to the PAG and PB, suggests that the LJA5 neurons may inhibit noxious sensory information. The presence of LJA5 neurons in human brainstems and their potential to inhibit noxious sensations highlights the translational relevance of this work in developing novel analgesic and anti-pruritic treatments. Furthermore, we show that LJA5 neurons receive input from forebrain structures implicated in stress and sensory detection. Therefore, we propose an adaptive role for the LJA5 neurons which may inhibit distracting noxious sensations under stressful conditions.

CONFLICT OF INTEREST

The authors have no conflict of interest to declare, they must also state this at submission.

DATA AVAILABILITY STATEMENT

The data that support the findings of this study are available from the corresponding author upon reasonable request.

ORCID

Lindsay J. Agostinelli https://orcid.org/0000-0002-8382-6638
Marco M. Hefti https://orcid.org/0000-0002-3127-4528

REFERENCES

Agostinelli, L. J., Geerling, J. C., & Scammell, T. E. (2019). Basal forebrain subcortical projections. _Brain Structure & Function_, _224_(3), 1097–1117. https://doi.org/10.1007/s00429-018-01820-6

Akil, H., Mayer, D. J., & Liebeskind, J. C. (1976). Antagonism of stimulation-produced analgesia by naloxone, a narcotic antagonist. _Science_, _191_(4230), 961–962. https://doi.org/10.1126/science.1251210

Amit, Z., & Galina, Z. H. (1988). Stress induced analgesia plays an adaptive role in the organization of behavioral responding. _Brain Research Bulletin_, _21_(6), 955–958. https://doi.org/10.1016/0361-9230(88)90033-0

Ansonoff, M. A., Zhang, J., Czyzyk, T., Rothman, R. B., Stewart, J., Xu, H., … Pintar, J. E. (2006). Antinociceptive and hypothermic effects of Salvinorin A are abolished in a novel strain of kappa-opioid receptor-1 knockout mice. _The Journal of Pharmacology and Experimental Therapeutics_, _318_(2), 641–648. https://doi.org/10.1124/jpet.106.101998

Barik, A., Thompson, J. H., Seltzer, M., Ghitani, N., & Chesler, A. T. (2018). A brainstem-spinal circuit controlling nocifensive behavior. _Neuron_, _100_(6), 1491–1503 e1493. https://doi.org/10.1016/j.neuron.2018.10.037

Bernard, J. F., Dallel, R., Raboisson, P., Villanueva, L., & Le Bars, D. (1995). Organization of the efferent projections from the spinal cervical enlargement to the parabrachial area and periaqueductal gray: A PHA-L study in the rat. _The Journal of Comparative Neurology_, _353_(4), 480–505. https://doi.org/10.1002/cne.903530403

Bester, H., Chapman, V., Besson, J. M., & Bernard, J. F. (2000). Physiological properties of the lamina I spinoparabrachial neurons in the rat. _Journal of Neurophysiology_, _83_(4), 2239–2259. https://doi.org/10.1152/jn.2000.83.4.2239

Bruinstroop, E., Cano, G., Vanderhorst, V. G., Cavalcante, J. C., Wirth, J., Sena-Esteves, M., & Saper, C. B. (2012). Spinal projections of the A5, A6 (locus coeruleus), and A7 noradrenergic cell groups in rats. _The Journal of Comparative Neurology_, _520_(9), 1985–2001. https://doi.org/10.1002/cne.23024

Byrum, C. E., & Guyenet, P. G. (1987). Afferent and efferent connections of the A5 noradrenergic cell group in the rat. _The Journal of Comparative Neurology_, _261_(4), 529–542. https://doi.org/10.1002/cne.902610406

Cameron, A. A., Khan, I. A., Westlund, K. N., & Willis, W. D. (1995). The efferent projections of the periaqueductal gray in the rat: A Phaseolus vulgaris-leucoagglutinin study. II. Descending projections. _The Journal of Comparative Neurology_, _351_(4), 585–601. https://doi.org/10.1002/cne.903510408

Campos, C. A., Bowen, A. J., Roman, C. W., & Palmiter, R. D. (2018). Encoding of danger by parabrachial CGRP neurons. _Nature_, _555_(7698), 617–622. https://doi.org/10.1038/nature25511

Cechetto, D. F., Standaert, D. G., & Saper, C. B. (1985). Spinal and trigeminal dorsal horn projections to the parabrachial nucleus in the rat. _The Journal of Comparative Neurology_, _240_(2), 153–160. https://doi.org/10.1002/cne.902400205

Clark, F. M., & Proudfit, H. K. (1993). The projections of noradrenergic neurons in the A5 catecholamine cell group to the spinal cord in the rat: Anatomical evidence that A5 neurons modulate nociception. _Brain Research_, _616_(1–2), 200–210. https://doi.org/10.1016/0006-8993(93)90210-e

Craig, A. D. (1995). Distribution of brainstem projections from spinal lamina I neurons in the cat and the monkey. _The Journal of Comparative Neurology_, _361_(2), 225–248. https://doi.org/10.1002/cne.903610204

Craig, A. D. (2002). How do you feel? Interoception: The sense of the physiological condition of the body. _Nature Reviews. Neuroscience_, _3_(8), 655–666. https://doi.org/10.1038/nrn894

Craig, A. D. (2009). How do you feel now? The anterior insula and human awareness. _Nature Reviews. Neuroscience_, _10_(1), 59–70. https://doi.org/10.1038/nrn2555

Dong, X., & Dong, X. (2018). Peripheral and central mechanisms of itch. _Neuron_, _98_(3), 482–494. https://doi.org/10.1016/j.neuron.2018.03.023

Fagius, J., Karhuvaara, S., & Sundlof, G. (1989). The cold pressor test: Effects on sympathetic nerve activity in human muscle and skin nerve fascicles. _Acta Physiologica Scandinavica_, _137_(3), 325–334. https://doi.org/10.1111/j.1748-1716.1989.tb08760.x

Fallon, J. H., & Leslie, F. M. (1986). Distribution of dynorphin and enkephalin peptides in the rat brain. _The Journal of Comparative Neurology_, _249_(3), 293–336. https://doi.org/10.1002/cne.902490302

Fields, H. L., Heinricher, M. M., & Mason, P. (1991). Neurotransmitters in nociceptive modulatory circuits. _Annual Review of Neuroscience_, _14_, 219–245. https://doi.org/10.1146/annurev.ne.14.030191.001251

Fitzek, S., Baumgartner, U., Marx, J., Joachimski, F., Axer, H., Witte, O. W., & Fitzek, C. (2006). Pain and itch in Wallenberg's syndrome: Anatomical-functional correlations. _Supplements to Clinical Neurophysiology_, _58_, 187–194.

Fodor, M, Gorcs, T J, & Palkovits, M. (1992). Immunohistochemical study on the distribution of neuropeptides within the pontine tegmentum--particularly the parabrachial nuclei and the locus coeruleus of the human brain. _Neuroscience_, _46_(4), 891–908.

Gao, Z. R., Chen, W. Z., Liu, M. Z., Chen, X. J., Wan, L., Zhang, X. Y., … Sun, Y. G. (2019). Tac1-expressing neurons in the periaqueductal Gray facilitate the itch-scratching cycle via descending regulation. _Neuron_, _101_(1), 45–59 e49. https://doi.org/10.1016/j.neuron.2018.11.010

Geerling, J. C., Kim, M., Mahoney, C. E., Abbott, S. B., Agostinelli, L. J., Garfield, A. S., … Scammell, T. E. (2016). Genetic identity of thermosensory relay neurons in the lateral parabrachial nucleus. _American Journal of Physiology. Regulatory, Integrative and Comparative Physiology_, _310_(1), R41–R54. https://doi.org/10.1152/ajpregu.00094.2015

Gogolla, N. (2017). The insular cortex. *Current Biology*, 27(12), R580–R586. https://doi.org/10.1016/j.cub.2017.05.010

Gordon, F. J., & McCann, L. A. (1988). Pressor responses evoked by micro-injections of L-glutamate into the caudal ventrolateral medulla of the rat. *Brain Research*, 457(2), 251–258. https://doi.org/10.1016/0006-8993(88)90693-2

Han, S., Soleiman, M. T., Soden, M. E., Zweifel, L. S., & Palmiter, R. D. (2015). Elucidating an affective pain circuit that creates a threat memory. *Cell*, 162(2), 363–374. https://doi.org/10.1016/j.cell.2015.05.057

Harris, J. A., Chang, P. C., & Drake, C. T. (2004). Kappa opioid receptors in rat spinal cord: Sex-linked distribution differences. *Neuroscience*, 124(4), 879–890. https://doi.org/10.1016/j.neuroscience.2003.12.042

Helmstetter, F. J., & Bellgowan, P. S. (1993). Lesions of the amygdala block conditional hypoalgesia on the tail flick test. *Brain Research*, 612(1–2), 253–257. https://doi.org/10.1016/0006-8993(93)91669-j

Huang, T., Lin, S. H., Malewicz, N. M., Zhang, Y., Zhang, Y., Goulding, M., … Ma, Q. (2019). Identifying the pathways required for coping behaviours associated with sustained pain. *Nature*, 565(7737), 86–90. https://doi.org/10.1038/s41586-018-0793-8

Hylden, J. L., Anton, F., & Nahin, R. L. (1989). Spinal lamina I projection neurons in the rat: Collateral innervation of parabrachial area and thalamus. *Neuroscience*, 28(1), 27–37. https://doi.org/10.1016/0306-4522(89)90229-7

Inan, S., & Cowan, A. (2004). Kappa opioid agonists suppress chloroquine-induced scratching in mice. *European Journal of Pharmacology*, 502(3), 233–237. https://doi.org/10.1016/j.ejphar.2004.09.010

Jankord, R., & Herman, J. P. (2008). Limbic regulation of hypothalamo-pituitary-adrenocortical function during acute and chronic stress. *Annals of the new York Academy of Sciences*, 1148, 64–73. https://doi.org/10.1196/annals.1410.012

Kapp, B. S., Schwaber, J. S., & Driscoll, P. A. (1985). The organization of insular cortex projections to the amygdaloid central nucleus and autonomic regulatory nuclei of the dorsal medulla. *Brain Research*, 360(1–2), 355–360. https://doi.org/10.1016/0006-8993(85)91254-5

Kardon, A. P., Polgar, E., Hachisuka, J., Snyder, L. M., Cameron, D., Savage, S., … Ross, S. E. (2014). Dynorphin acts as a neuromodulator to inhibit itch in the dorsal horn of the spinal cord. *Neuron*, 82(3), 573–586. https://doi.org/10.1016/j.neuron.2014.02.046

Kivell, B., & Prisinzano, T. E. (2010). Kappa opioids and the modulation of pain. *Psychopharmacology*, 210(2), 109–119. https://doi.org/10.1007/s00213-010-1819-6

Krashes, M. J., Shah, B. P., Madara, J. C., Olson, D. P., Strochlic, D. E., Garfield, A. S., … Lowell, B. B. (2014). An excitatory paraventricular nucleus to AgRP neuron circuit that drives hunger. *Nature*, 507(7491), 238–242. https://doi.org/10.1038/nature12956

Kumagai, H., Ebata, T., Takamori, K., Miyasato, K., Muramatsu, T., Nakamoto, H., … Suzuki, H. (2012). Efficacy and safety of a novel k-agonist for managing intractable pruritus in dialysis patients. *American Journal of Nephrology*, 36(2), 175–183. https://doi.org/10.1159/000341268

Liebeskind, J. C., Guilbaud, G., Besson, J. M., & Oliveras, J. L. (1973). Analgesia from electrical stimulation of the periaqueductal gray matter in the cat: Behavioral observations and inhibitory effects on spinal cord interneurons. *Brain Research*, 50(2), 441–446. https://doi.org/10.1016/0006-8993(73)90748-8

Light, A. R., Sedivec, M. J., Casale, E. J., & Jones, S. L. (1993). Physiological and morphological characteristics of spinal neurons projecting to the parabrachial region of the cat. *Somatosensory & Motor Research*, 10(3), 309–325.

Madden, J. t., Akil, H., Patrick, R. L., & Barchas, J. D. (1977). Stress-induced parallel changes in central opioid levels and pain responsiveness in the rat. *Nature*, 265(5592), 358–360. https://doi.org/10.1038/265358a0

Maixner, W., Gracely, R. H., Zuniga, J. R., Humphrey, C. B., & Bloodworth, G. R. (1990). Cardiovascular and sensory responses to forearm ischemia and dynamic hand exercise. *The American Journal of Physiology*, 259(6 Pt 2), R1156–R1163. https://doi.org/10.1152/ajpregu.1990.259.6.R1156

Mansfield, K. E., Sim, J., Jordan, J. L., & Jordan, K. P. (2016). A systematic review and meta-analysis of the prevalence of chronic widespread pain in the general population. *Pain*, 157(1), 55–64. https://doi.org/10.1097/j.pain.0000000000000314

Merchenthaler, I., Maderdrut, J. L., Cianchetta, P., Shughrue, P., & Bronstein, D. (1997). In situ hybridization histochemical localization of prodynorphin messenger RNA in the central nervous system of the rat. *The Journal of Comparative Neurology*, 384(2), 211–232.

Millan, M. J. (2002). Descending control of pain. *Progress in Neurobiology*, 66(6), 355–474.

Moga, M. M., Herbert, H., Hurley, K. M., Yasui, Y., Gray, T. S., & Saper, C. B. (1990). Organization of cortical, basal forebrain, and hypothalamic afferents to the parabrachial nucleus in the rat. *The Journal of Comparative Neurology*, 295(4), 624–661. https://doi.org/10.1002/cne.902950408

Moss, M. S., & Basbaum, A. I. (1983). The peptidergic organization of the cat periaqueductal gray. II. The distribution of immunoreactive substance P and vasoactive intestinal polypeptide. *The Journal of Neuroscience*, 3(7), 1437–1449.

Mu, D., Deng, J., Liu, K. F., Wu, Z. Y., Shi, Y. F., Guo, W. M., … Sun, Y. G. (2017). A central neural circuit for itch sensation. *Science*, 357(6352), 695–699. https://doi.org/10.1126/science.aaf4918

Neuhuber, W. (1982). The central projections of visceral primary afferent neurons of the inferior mesenteric plexus and hypogastric nerve and the location of the related sensory and preganglionic sympathetic cell bodies in the rat. *Anatomy and Embryology*, 164(3), 413–425.

Neuhuber, W. L., & Sandoz, P. A. (1986). Vagal primary afferent terminals in the dorsal motor nucleus of the rat: Are they making monosynaptic contacts on preganglionic efferent neurons? *Neuroscience Letters*, 69(2), 126–130. https://doi.org/10.1016/0304-3940(86)90590-2

Nordin, M., & Fagius, J. (1995). Effect of noxious stimulation on sympathetic vasoconstrictor outflow to human muscles. *The Journal of Physiology*, 489(Pt 3), 885–894. https://doi.org/10.1113/jphysiol.1995.sp021101

Oaklander, A. L. (2012). Common neuropathic itch syndromes. *Acta Dermato-Venereologica*, 92(2), 118–125. https://doi.org/10.2340/00015555-1318

Ortiz, J. P., Close, L. N., Heinricher, M. M., & Selden, N. R. (2008). Alpha(2)-noradrenergic antagonist administration into the central nucleus of the amygdala blocks stress-induced hypoalgesia in awake behaving rats. *Neuroscience*, 157(1), 223–228. https://doi.org/10.1016/j.neuroscience.2008.08.051

Panneton, W. M., & Burton, H. (1985). Projections from the paratrigeminal nucleus and the medullary and spinal dorsal horns to the peribrachial area in the cat. *Neuroscience*, 15(3), 779–797. https://doi.org/10.1016/0306-4522(85)90078-8

Reynolds, D. V. (1969). Surgery in the rat during electrical analgesia induced by focal brain stimulation. *Science*, 164(3878), 444–445. https://doi.org/10.1126/science.164.3878.444

Rodriguez, E., Sakurai, K., Xu, J., Chen, Y., Toda, K., Zhao, S., … Wang, F. (2017). A craniofacial-specific monosynaptic circuit enables heightened affective pain. *Nature Neuroscience*, 20(12), 1734–1743. https://doi.org/10.1038/s41593-017-0012-1

Roesler, R., & Schwartsmann, G. (2012). Gastrin-releasing peptide receptors in the central nervous system: Role in brain function and as a drug target. *Frontiers in Endocrinology (Lausanne)*, 3, 159. https://doi.org/10.3389/fendo.2012.00159

Samineni, V. K., Grajales-Reyes, J. G., Copits, B. A., O'Brien, D. E., Trigg, S. L., Gomez, A. M., … Gereau, R. W. t. (2017). Divergent modulation of nociception by Glutamatergic and GABAergic neuronal subpopulations in the periaqueductal Gray. *eNeuro*, 4(2), ENEURO.0129–ENEU16.2017. https://doi.org/10.1523/ENEURO.0129-16.2017

Saper, C. B., & Petito, C. K. (1982). Correspondence of melanin-pigmented neurons in human brain with A1-A14 catecholamine cell groups. *Brain*, *105*(Pt 1), 87–101. https://doi.org/10.1093/brain/105.1.87

Schaefer, C., Sadosky, A., Mann, R., Daniel, S., Parsons, B., Tuchman, M., … Nieshoff, E. (2014). Pain severity and the economic burden of neuropathic pain in the United States: BEAT neuropathic pain observational study. *ClinicoEconomics and Outcomes Research*, *6*, 483–496. https://doi.org/10.2147/CEOR.S63323

Sikandar, S., West, S. J., McMahon, S. B., Bennett, D. L., & Dickenson, A. H. (2017). Sensory processing of deep tissue nociception in the rat spinal cord and thalamic ventrobasal complex. *Physiological Reports*, *5*(14), e13323. https://doi.org/10.14814/phy2.13323

Standaert, D. G., Watson, S. J., Houghten, R. A., & Saper, C. B. (1986). Opioid peptide immunoreactivity in spinal and trigeminal dorsal horn neurons projecting to the parabrachial nucleus in the rat. *The Journal of Neuroscience*, *6*(5), 1220–1226.

Sun, W., & Panneton, W. M. (2002). The caudal pressor area of the rat: Its precise location and projections to the ventrolateral medulla. *American Journal of Physiology. Regulatory, Integrative and Comparative Physiology*, *283*(3), R768–R778. https://doi.org/10.1152/ajpregu.00184.2002

Sun, W., & Panneton, W. M. (2005). Defining projections from the caudal pressor area of the caudal ventrolateral medulla. *The Journal of Comparative Neurology*, *482*(3), 273–293. https://doi.org/10.1002/cne.20434

Sun, Y. G., & Chen, Z. F. (2007). A gastrin-releasing peptide receptor mediates the itch sensation in the spinal cord. *Nature*, *448*(7154), 700–703. https://doi.org/10.1038/nature06029

Sun, Y. G., Zhao, Z. Q., Meng, X. L., Yin, J., Liu, X. Y., & Chen, Z. F. (2009). Cellular basis of itch sensation. *Science*, *325*(5947), 1531–1534. https://doi.org/10.1126/science.1174868

Tokita, K., Inoue, T., & Boughter, J. D., Jr. (2009). Afferent connections of the parabrachial nucleus in C57BL/6J mice. *Neuroscience*, *161*(2), 475–488. https://doi.org/10.1016/j.neuroscience.2009.03.046

Veinante, P., Yalcin, I., & Barrot, M. (2013). The amygdala between sensation and affect: A role in pain. *Journal of Molecular Psychiatry*, *1*(1), 9. https://doi.org/10.1186/2049-9256-1-9

Verstegen, A. M. J., Vanderhorst, V., Gray, P. A., Zeidel, M. L., & Geerling, J. C. (2017). Barrington's nucleus: Neuroanatomic landscape of the mouse "pontine micturition center". *The Journal of Comparative Neurology*, *525*(10), 2287–2309. https://doi.org/10.1002/cne.24215

Wada, E., Way, J., Lebacq-Verheyden, A. M., & Battey, J. F. (1990). Neuromedin B and gastrin-releasing peptide mRNAs are differentially distributed in the rat nervous system. *The Journal of Neuroscience*, *10*(9), 2917–2930.

Waldhoer, M., Bartlett, S. E., & Whistler, J. L. (2004). Opioid receptors. *Annual Review of Biochemistry*, *73*, 953–990. https://doi.org/10.1146/annurev.biochem.73.011303.073940

Wikstrom, B., Gellert, R., Ladefoged, S. D., Danda, Y., Akai, M., Ide, K., … Ueno, Y. (2005). Kappa-opioid system in uremic pruritus: Multicenter, randomized, double-blind, placebo-controlled clinical studies. *Journal of the American Society of Nephrology*, *16*(12), 3742–3747. https://doi.org/10.1681/ASN.2005020152

Yeung, J. C., Yaksh, T. L., & Rudy, T. A. (1977). Concurrent mapping of brain sites for sensitivity to the direct application of morphine and focal electrical stimulation in the production of antinociception in the rat. *Pain*, *4*(1), 23–40. https://doi.org/10.1016/0304-3959(77)90084-7

Yin, J. B., Wu, H. H., Dong, Y. L., Zhang, T., Wang, J., Zhang, Y., … Li, Y. Q. (2014). Neurochemical properties of BDNF-containing neurons projecting to rostral ventromedial medulla in the ventrolateral periaqueductal gray. *Frontiers in Neural Circuits*, *8*, 137. https://doi.org/10.3389/fncir.2014.00137

Yosipovitch, G., & Bernhard, J. D. (2013). Clinical practice. Chronic pruritus. *The New England Journal of Medicine*, *368*(17), 1625–1634. https://doi.org/10.1056/NEJMcp1208814